XXI International Congress of the Carpathian Balkan Geological Association (CBGA 2018)
Berichte der Geologischen Bundesanstalt, v. 126, p. 47 – 80

Field Trip Pre-EX-2

Sedimentary and tectonic processes on a Late Jurassic passive margin and its inversion during Alpine orogeny in the Lofer area

HUGO ORTNER[1], DIETHARD SANDERS[1], MICHAELA USTASZEWSKI[1,2], MARTIN RITTNER[1,3], DAVID MOSNA[1,4] & SEBASTIAN WOLFGRUBER[1,5]

[1] Institut für Geologie, Universität Innsbruck, Innrain 52, 6020 Innsbruck, Austria. hugo.ortner@uibk.ac.at
[2] Von-Hase-Weg 15, 07743 Jena, Germany. michaust@gmail.com
[3] Tofwerk AG, Uttigenstrasse 22, 3600 Thun, Switzerland. rittner@tofwerk.com
[4] Amt für Geologie und Baustoffprüfung, Eggentaler Straße 48, 39053 Kardaun, Italy. david.mosna@provinz.bz.it
[5] Schenker Richter Graf AG, Büttenenhalde 42, 6006 Luzern, Switzerland. sebastian.wolfgruber@fsgeolog.ch

Introduction

The geology of the area around Lofer inspired the Bavarian geologist Felix Hahn to subdivide the Northern Calcareous Alps (NCA) tectonically (HAHN, 1912, 1913b). This subdivision was adopted by, e.g., TOLLMANN (1976b, 1985) and is essentially still in use. The clear relationships between some of the major tectonic units of the NCA is our motivation to do this field trip.

The NCA evolved through several geodynamic stages. In the Triassic, the future NCA formed the southeastern passive margin of Pangea (including present-day Europe) toward the Meliata ocean (e.g., HAAS et al., 1995; STAMPFLI & BOREL, 2002), where a thick succession of carbonates accumulated. Liassic rifting opened the Alpine Tethys ocean and separated the Adriatic plate fragment from the European plate (e.g., HANDY et al., 2010). This created a new continental margin that is well developed in the western part of Adria-derived tectonic units in eastern Switzerland and western Austria (FROITZHEIM & MANATSCHAL, 1996; LAVIER & MANATSCHAL, 2006). In the Late Jurassic, Neotethys oceanic crust had been obducted onto the southeastern margin of the Adriatic plate (SCHMID et al., 2008; SCHMID et al., 2004), however, it is unclear how far this obduction extended into the NCA. During the Cretaceous, the NCA formed as typical foreland fold-and-thrust belt in the external part of the mountain belt that evolved as a consequence of the closure of a part of the Neotethys ocean (e.g., ORTNER et al., 2016). Collision within this belt started during the Early Cretaceous. Probably obduction and collision on one side and rifting and drifting on the other side of the Adriatic plate were kinematically linked by a system of transform faults that crossed the Adriatic plate (TRÜMPY, 1988; WEISSERT & BERNOULLI, 1985). Closure of the Alpine Tethys and subsequent collision during the Cenozoic caused a second orogenic cycle during which the NCA were passively transported piggy-back into the European foreland. In the late stages of this event, the geometry of the NCA thrust sheets was modified by escape tectonics, when orogenically thickened crust moved east toward the Pannonian basin (RATSCHBACHER et al., 1991; ROSENBERG et al., 2007). The NCA were dissected by NE to ENE-striking subvertical strike-slip faults, some with tens of kilometers offset (DECKER et al., 1994; LINZER et al., 2002; PERESSON & DECKER, 1997) that delimited the eastward moving units agains more stable units to the north. However, some of the steep faults near the northern margin of the NCA are rather tear faults related to incorporation and emplacement of

the Helvetic and Subalpine Molasse during oblique convergence between the Alpine wedge and the European foreland (ORTNER et al., 2015).

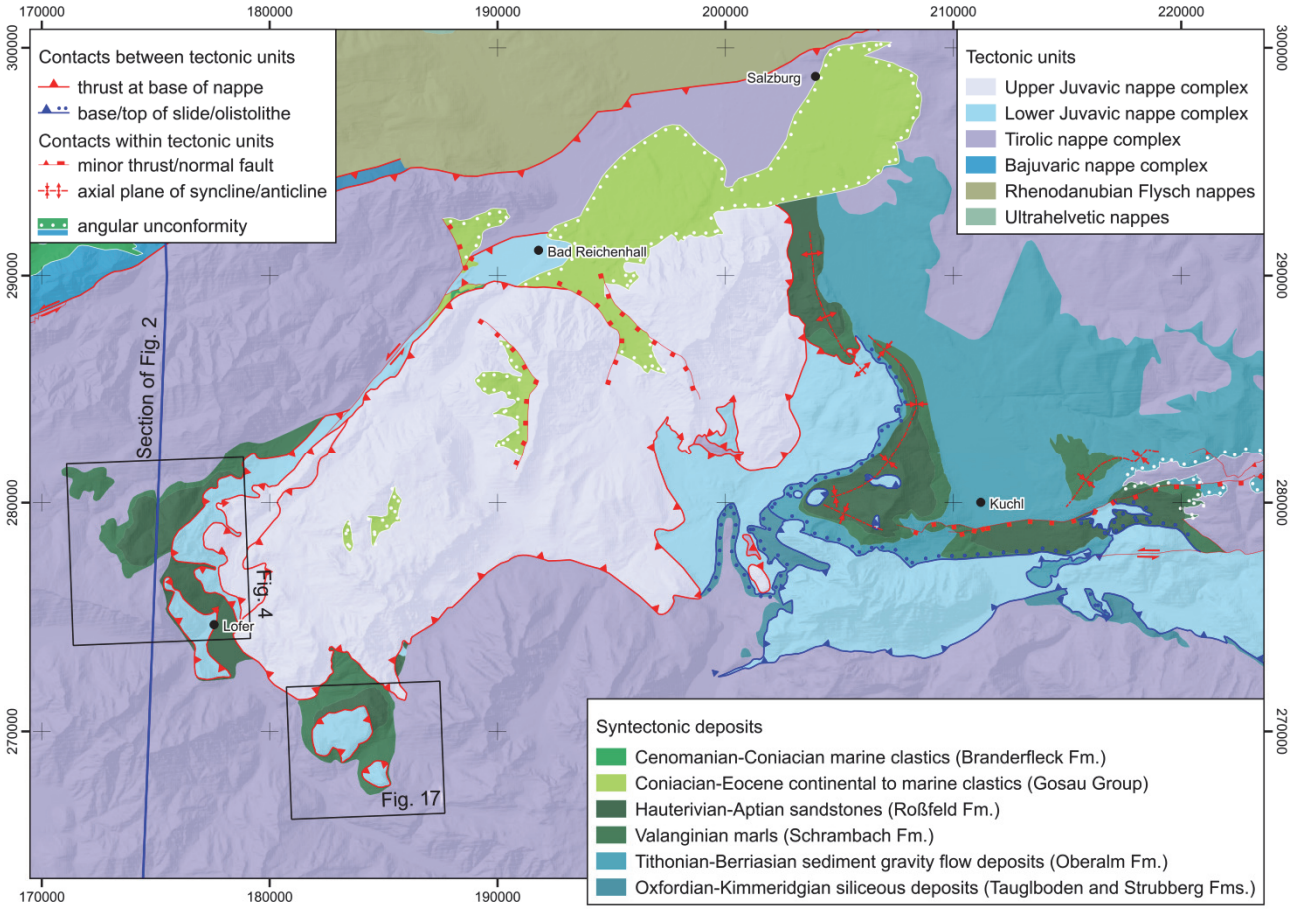

Fig. 1: Tectonic map including syntectonic sediments of the field trip area around Lofer, following the tectonic subdivision of TOLLMANN (1976b). Tectonic boundaries were drawn using also unconformities between tectonic units, which is the case when large olistolithes are emplaced and later covered (ORTNER, 2017b).

As mentioned above, the NCA fold-and-thrust belt formed initially in the late Early Cretaceous. Timing of thrust movements can be deduced from the youngest sediments below a thrusted unit, as shortening was active in a deep-water environment and non-deposition would have left hardgrounds (ORTNER, 2003). Using this argument, two emplacement processes on top of the Tirolic nappe complex can be distinguished: (1) emplacement of the Lower Juvavic unit onto sediments of Oxfordian-Kimmeridgian age (Fig. 1, S and SE of Kuchl), and (2) emplacement of the Lower and Upper Juvavic units onto Aptian deposits (Fig. 1, N and SE of Lofer).

The purpose of this field trip is to showcase several steps of this evolution. During the two days of the field trip we will address following problems:

- The Jurassic sedimentary evolution of the NCA and the relevance of the Upper Jurassic transgression in the Central part of the NCA.
- The controversially discussed Upper Jurassic tectonic evolution of the NCA – Jurassic orogeny within the NCA (e.g., GAWLICK et al., 1999; MISSONI & GAWLICK, 2010) versus passive margin affected by transform faults (FRANK & SCHLAGER, 2006; ORTNER et al., 2008).
- The pattern of young (Miocene) faults that dissects the pre-existing nappe stack

The field trip is led by H. Ortner and D. Sanders. It takes place in an Alpine landscape and is strongly dependent on weather conditions, and changing outcrop conditions. The succession and number of stops may be changed on short notice.

Field Trip

Day 1 - Unkenbachtal: Stops 1 to 4

The Unkenbachtal is the valley of the Unkenbach and a northern tributary of the Saalach. It lies within the northern limb of the Unken syncline (Fig. 2), which is open and roughly ENE-WSW-trending. The Unkenbachtal exposes the complete Jurassic to Cretaceous sedimentary succession of the Staufen-Höllengebirgs thrust sheet of the Tirolic nappe complex, including the Schwarzbergklamm breccia. We will start at the base of the sedimentary succession in the western part of the valley and go into progressively younger sediments toward the outer, eastern end. The main idea of this part of the field trip is to show the Jurassic to Cretaceous succession (Fig. 3).

The Schwarzbergklamm breccia is „chaotic, clast- to matrix-supported and lacks any kind of sorting. The matrix consists of red calcareous micrite. The clasts are angular to sub-angular and consist mainly of Upper Rhaetian limestone, subordinately of Dachstein limestone, marls of the Kössen Formation, red limestones of the Adnet and Klaus Formations and the Ruhpolding Radiolarite. Clast sizes range from a few millimetres to several meters in diameter. Single blocks measure up to 40 meters“ (ORTNER et al., 2008). It attracted the attention of several workers, who gave a wide range of interpretations reaching from tectonic breccias (VORTISCH, 1931) to submarine mass transport deposits (DIERSCHE, 1980; FISCHER, 1965; GARRISON & FISCHER, 1969; VECSEI et al., 1989; WÄCHTER, 1987).

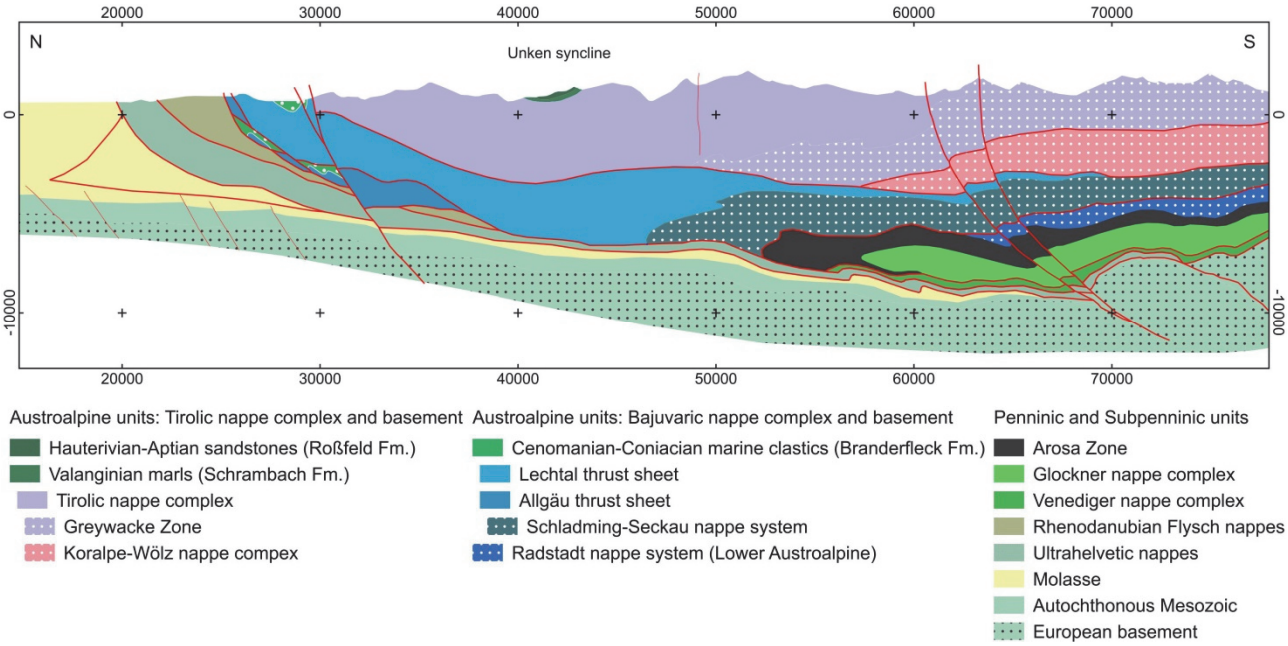

Fig. 2: Regional cross section of the NCA in the field trip area, simplified from BRAUNSTINGL (2005). See Fig. 1 for trace of section. Note the Unken syncline on the center of the section.

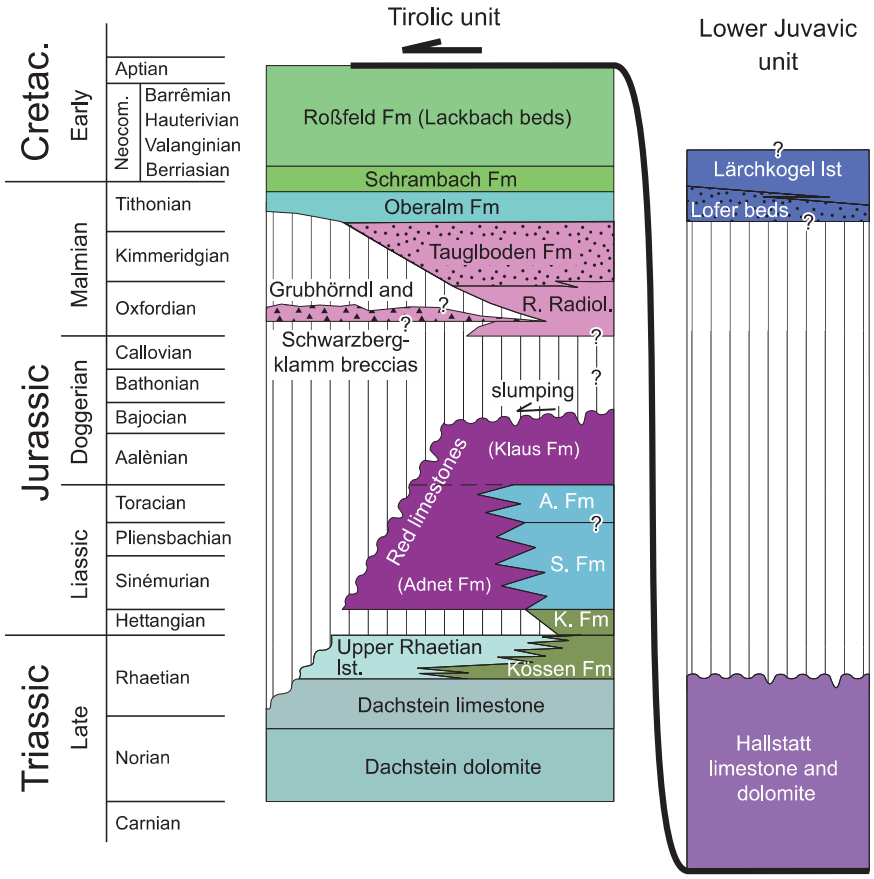

Fig. 3: Chronostratigraphic diagram for the Unken syncline, adapted from ORTNER et al. (2008). K. Fm = Kendlbach Formation, S. Fm = Scheibelberg Formation, A. Fm = Allgäu Formation, R. Radiol. = Ruhpolding Radiolarite, lst = limestone. Formal and informal subdivisions used in accordance with the Stratigrapic Chart of Austria (PILLER et al., 2004), except “Oberrhätkalk”, which is Upper Rhaetian limestone.

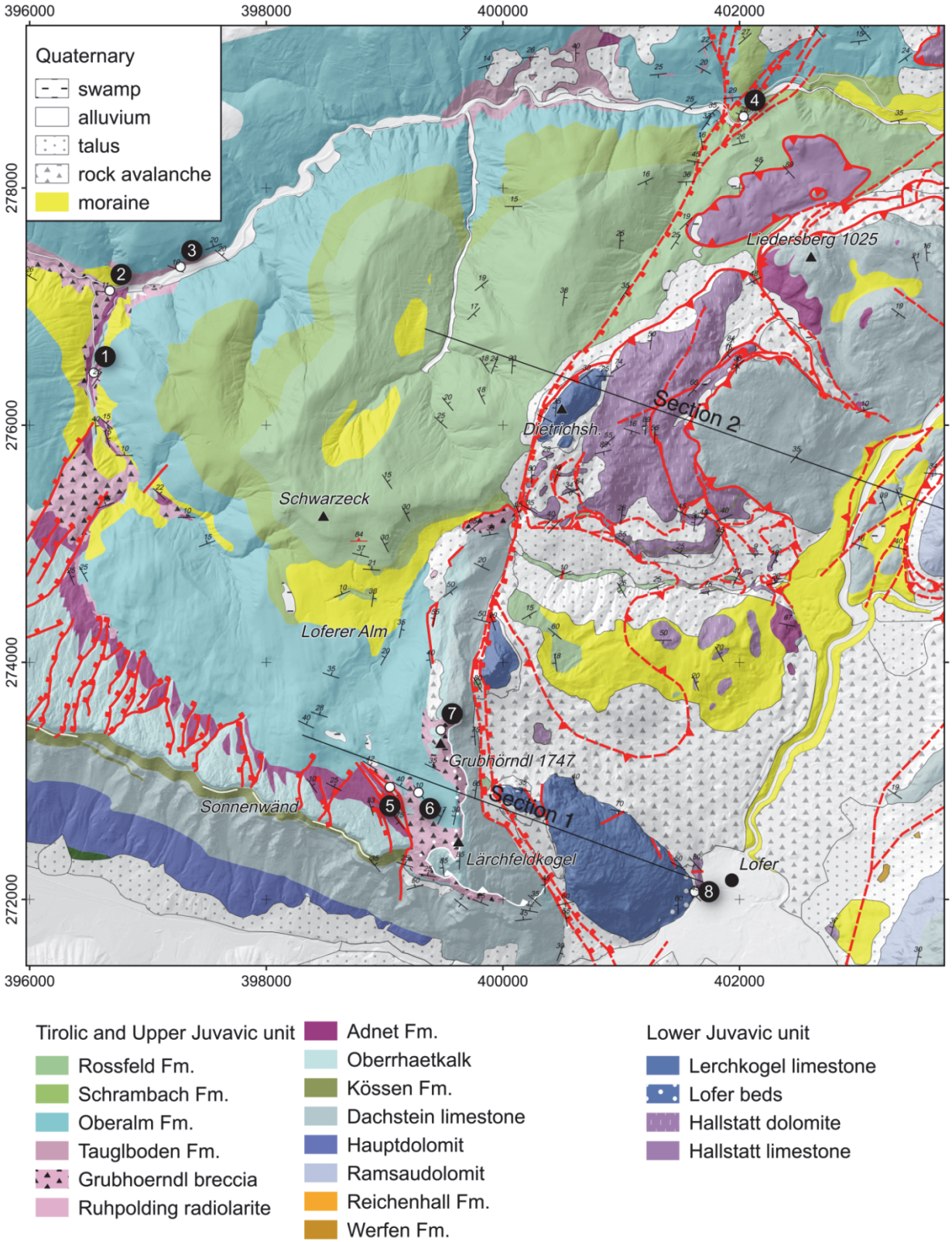

Fig. 4: Geologic map of the Unken syncline and the northwestern part of the Juvavic nappe complex, compiled from LUKESCH (2003) and RITTNER (2006), westernmost part from (HORNSTEINER, 1991). Minor modifications according to (PAVLIK, 2006). We do not follow GAWLICK et al. (2015) regarding the position of the Saalachtal-Westbruch. Numbers 1 – 8 indicate field trip stops of day 1. Sections are shown in Fig. 12. Coordinates: MGI Austria GK M31.shown in Fig. 12. Coordinates: MGI Austria GK M31.

Stop 1. Fußtal near game feeding place

Coordinates: E 12.62285, N 47.62064.
Altitude: 937 m.

At Stop 1 the erosive contact of the Schwarzbergklamm breccia to underlying red limestones of the Klaus Formation is exposed (Fig. 5). Within the breccia, large imbricated clasts can be seen. The red limestones overlie Upper Rhätian limestones in the vicinity of Stop 1.

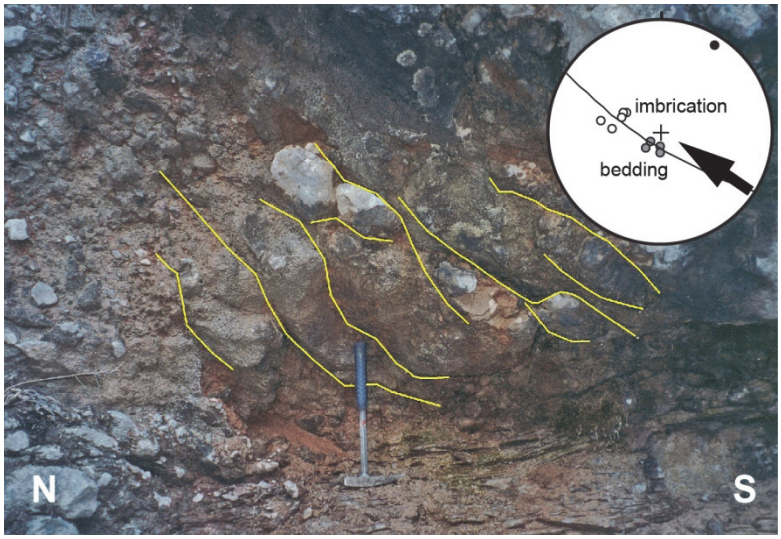

Fig. 5: Field photograph of detail in Stop1. Yellow lines emphasize bases of imbricated clasts near the base of the Schwarzbergklamm breccia. Inset shows poles to bedding (grey circles) and poles to imbricated clasts (white circles), and a common creat circle. The asymmetry of the data distribution indicates a local transport direction to the NW (black arrow). Length of hammer for scale is 42 cm.

Stop 2. Schwarzbergklamm

Coordinates: E 12.62261, N 47.63089.
Altitude: 771 m.

The Schwarzbergklamm offers the best outcrops of the Schwarzbergklamm breccia. The gorge is cut into a large block of Upper Rhaetian limestone within the breccia that has a minimum diameter of 40 m. The gorge can be accessed from its downstream end. There, the relationship of the breccia to the underlying deposits can be studied. At the innermost part of the accessible gorge, a part of the breccia underlying the block is in contact with Red limestones (Fig. 6a). The base of the breccia is irregular, and the underlying red limestones are cut by several shear planes cutting upsection into the breccia. The shear planes are seen to root in bedding planes. Bedding parallel shear did cause duplexing within the red limestones, and the topography related to the duplex causes the wavy base of the breccia. The shear planes are not discrete, and a foliation related to shearing is developed. At the time of deformation, neither the Red limestones nor the Schwarzbergklamm breccia were fully lithified. Bedding plane orientations within the duplex indicate a NNW-directed shear direction.

On the southern side of the outer part of the gorge, the breccia is seen between the Red limestones below, and the Ruhpolding radiolarite above, none of the contacts being erosive (Fig. 6b). On the northern side, however, the top of the red limestones cuts downsection and is locally covered by a thin, up to 10 cm thick band of cherts of the Ruhpolding radiolarite, which is in turn covered by the Schwarzbergklamm breccia (Fig. 6c).

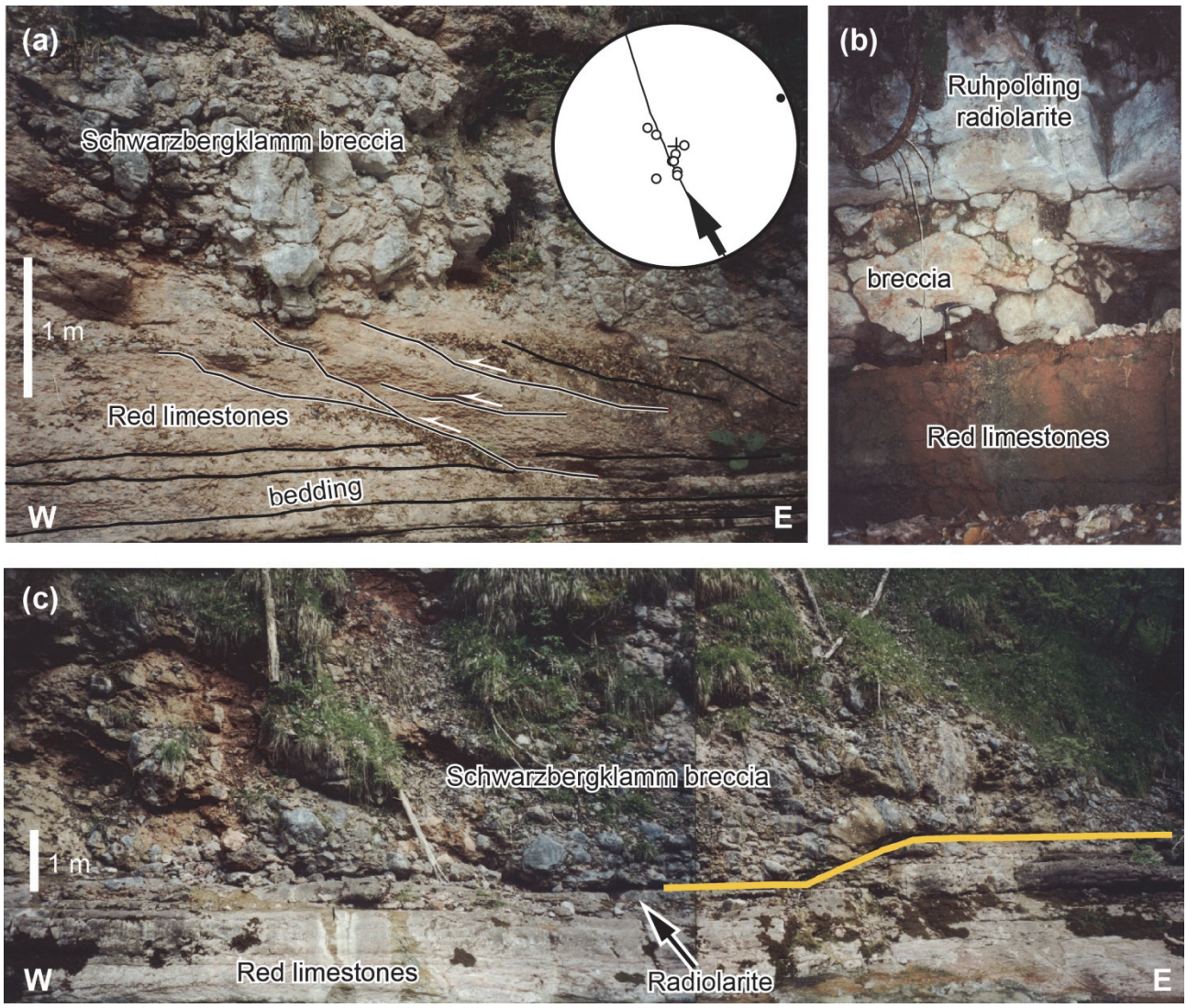

Fig. 6: Field photographs from the Schwarzbergklamm. (a) Shear structures at the base of the Schwarzbergklamm breccia. Inset: Poles to bedding in the Red limestones. The asymmetry and distribution along a great circle segment indicates top to NNW transport of the breccia. (b) At the south side of the outer gorge, the Schwarzbergklamm breccia is intercalated between Red limestones below, and the Ruhpolding radiolarite above. The basal contact is not erosive. (c) At the north side of the outer gorge, the base of the Schwarzbergklamm is lined by a thin discontinuous band of Ruhpolding radiolarite. Yellow line highlights this contact that cuts downsection into the Red limestones.

Based on these observations, the age of deposition of the Schwarzbergklamm breccia can be constrained to be during deposition of the Ruhpolding radiolarite (see Fig. 3). Locally parts of the Red limestones slumped away prior to breccia deposition sometime during the Lower or Middle Jurassic. At the time of deposition of the breccia, the Red limestones were not fully lithified. Emplacement of the breccia did cause bedding-parallel shear of the Red limestones, locally leading to duplexing and deformation of the base of the breccia.

Stop 3. 500 m east of Schwarzbergklamm

Coordinates: E 12.63058, N 47.63227.
Altitude: 745 m.

500 m east of the Geblfußalm, and roughly the same distance downstream from the Schwarzbergklamm gorge, the northern bank of the Unkenbach exposes the contact between the Tauglboden and Oberalm Formations The Tauglboden Formation develops gradually from the cherts of the Ruhpolding radiolarite by an increase in marl, intercalated with turbidites that redeposit radiolarians, and with some layers rich in lithoclasts (see, e.g., SCHLAGER & SCHLAGER, 1973; VECSEI et al., 1989). In contrast, the Oberalm Formation consists of an alternation of micritic to lutitic limestones with allodapic limestones („Barmstein limstones“) that transport bioclastic material, and some lithoclastic material into the deep sea (GARRISON & FISCHER, 1969; STEIGER, 1981).

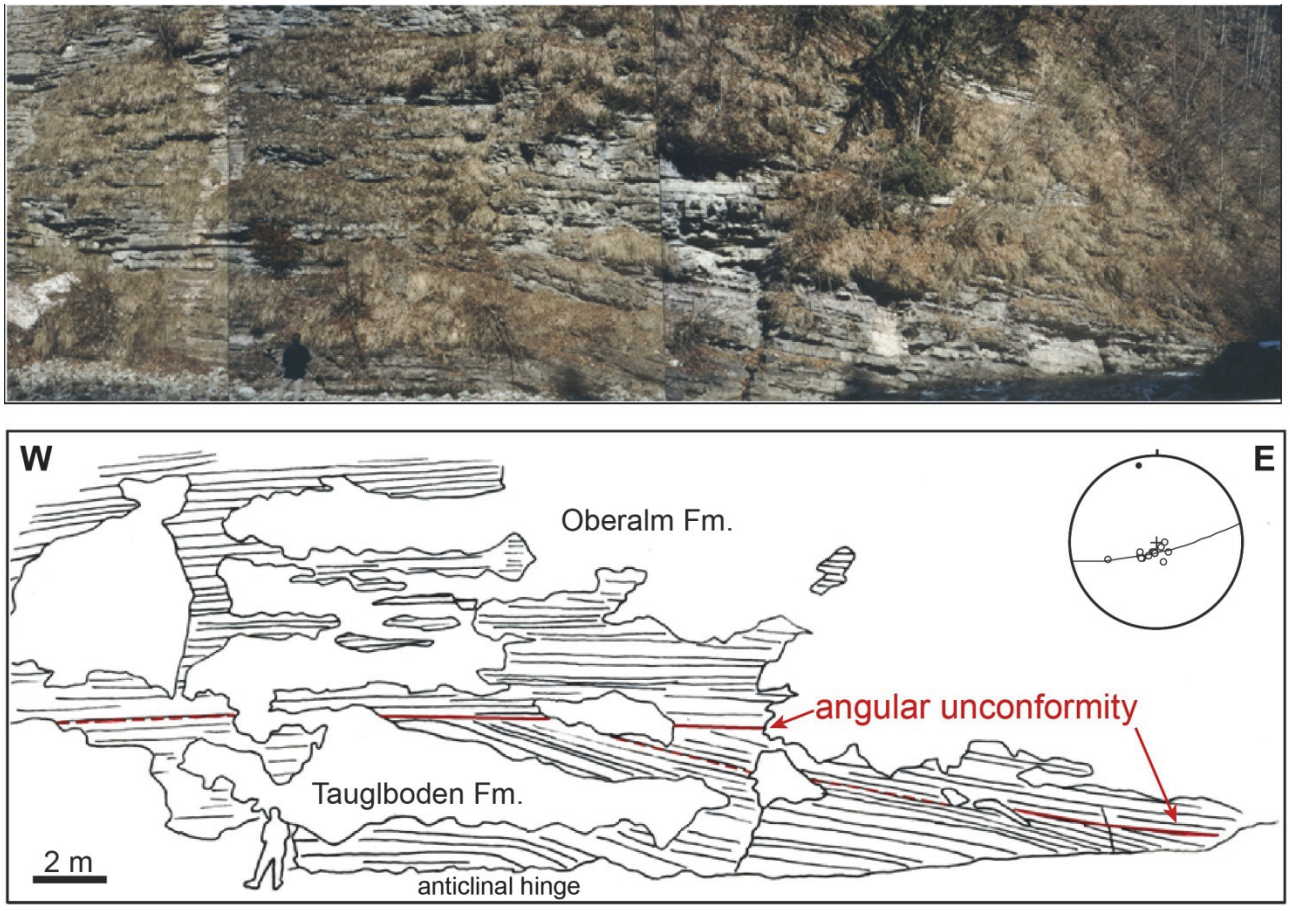

Fig. 7: Angular unconformity between Tauglboden und Oberalm Formations at Stop 3. Within the Tauglboden Formation, the hinge of an anticline is visible, tilting the beds in the eastern limb to the east. There, one or more angular unconformities within the Tauglboden Formation are present, depending on the detail of observation. Inset shows poles to bedding of the tilted beds.

The two sedimentary units are separated by an angular unconformity, increasing in angle from the anticlinal hinge to the east and downsection (Fig. 7). Beds below unconformities are tilted and truncated. Within the Tauglboden Formation, only minor wedging toward the fold hinge is visible, unconformities are related to erosion events that removed part of the sedimentary succession. The principal progressive unconformity, sensu FORD et al. (1997), where all unconformities merge, is the base of the Oberalm Formation The observed structures are compatible with progressive rollover in the hanging wall of a normal fault.

The geometry observed requires a listric fault rollover. The narrow anticlinal hinge allows to estimate the depth of detachment, which is probably not deeper than a few tens of meters below surface, and this probably within the Red limestones.

Stop 4. Friedlwirt

Coordinates: E 12.69434, N 47.64439.
Altitude: 628 m.

In the outer Unkenbachtal, the Cretaceous part of the sedimentary succession of the Unken syncline is exposed, which includes the youngest part of the Oberalm Formation, the Schrambach and Roßfeld Formations. The base of the Schrambach Formation is characterized by the end of the limestones of the Oberalm Formation, and the onset of a thick marl dominated succession (DARGA & WEIDICH, 1986; RASSER et al., 2003). The transition to the Roßfeld Formation is defined by the first sand rich beds (DECKER et al., 1987), and was described as Lackbach beds in the Unken syncline (DARGA & WEIDICH, 1986).

The Friedlwirt outcrop exposes a very coarse clastic part of the Roßfeld Formation, which is, according to DARGA & WEIDICH (1986), in the upper third of the succession. Rounded to well-rounded components with a diameter up to 15 cm float in a matrix of sandy marl. Most of the components are derived from the NCA, but also phyllites and quartz pebbles are found, and rare ultrabasites (DARGA & WEIDICH, 1986). The sediments are slumped, with slump fold axes in the S to SE and facing to the SW. This may indicate a SW-dipping paleoslope.

Day 1 – Loferer Alm: Stops 5 to 8

At Loferer Alm, the Grubhörndl breccia is exposed. The Grubhörndl breccia was described already at the begin of the 20th century („Buntes Rhät“, Hahn, 1910; „Gosaubreccia“; Ampferer, 1927), but its nature and the connection to the Schwarzbergklamm breccia was only recognized by ORTNER et al. (2008). The most spectacular feature of the Grubhörndl breccia is a mountain-sized olistolithe that is wrapped by the breccia on all sides (Fig. 8). Because of its large size, this olistolithe controlled the distribution of facies well into the Upper Jurassic.

We cross the Loferer Alm to the south from Haus Schönblick to reach the immediate vicinity of the Grubhörndl, passing a large area where the Oberalm Formation is exposed (Fig. 4).

Stop 5. West of Grubhörndl, eastern side of Urltal

Coordinates: E 12.65622, N 47.59333.

A hardground is exposed between Upper Rhaetian limestones and the Oberalm Formation As the Grubhörndl breccia is exposed in the surrounding, we suggest that the Upper Rhätian limestone is a large block in the breccia. Nevertheless the hardground documents long time spans of non-deposition on top of the breccia.

Stop 6. Western flank of Grubhörndl, near the end of a dirt road

Coordinates: E 12.65830, N 47.59287.
Altitude: 1535 m.

Here, Barmstein limestones of the Oberalm Formation directly overlie the Grubhörndl breccia. The boundary is a greenish hardground. The Barmstein limestones redeposit lithoclasts, e.g. from the Adnet Formation, and bioclasts, which include crinoids, bivalves, and rare large branched fragments of hydrozoans.

Stop 7. Summit of Grubhörndl

Coordinates: E 12.66105, N 47.59644.
Altitude: 1787 m.

A few meters below the ridge between Lärchfeldkopf and Grubhörndl, the contact between the Upper Rhätian limestone of the mega-olistolith and the Grubhörndl breccia is exposed. Bedding in the olistolith is vertical. The summit of Grubhörndl has a wide view in all directions, and at this point we will discuss some aspects of the geologic evolution of the area.

Toward the west, the view goes over the Waidringer Steinplatte and its famous reef in the Upper Rhaetian limestone. At the ridge toward the Strub valley, the top surface of this limestone has been excavated by erosion. It has an irregular surface (Fig. 4), that is controlled by a system of west-dipping normal faults. The faults cut the limestone into lozenge-shaped pieces that are limited by roughly N- and NNE-striking faults, however, no systematic cross cutting relationships are observed (Fig. 4). The faults are planar, perpendicular to bedding, and only few of them cut across the marls of the Kössen Formation, that underly the Upper Rhätian limestone and separate it from the Dachstein limestone (Figs. 4, 9). Upsection, the faults do offset the Red limestones and the Ruhpolding radiolarites, but they end near the base of the Oberalm Formation.

Therefore, the timing of these normal faults and deposition of the Schwarzbergklamm and Grubhörndl breccias is comparable. The breccias and the normal faults postdate the Red limestones, and predate the Oberalm Formation As most of the normal faults do not cut down to the Dachstein limestone, the Upper Rhätian limestone must have décolled on top of the Kössen Formation The faults probably originated as tension joints orthogonal to bedding, and then rotated in a domino style. West-directed transport of the Upper Rhätian limestone was associated with 6-12% stretching (Ortner et al., 2008). The two conjugate fault sets indicate non-plane strain during joint initiation (e.g., Reches & Dieterich, 1983).

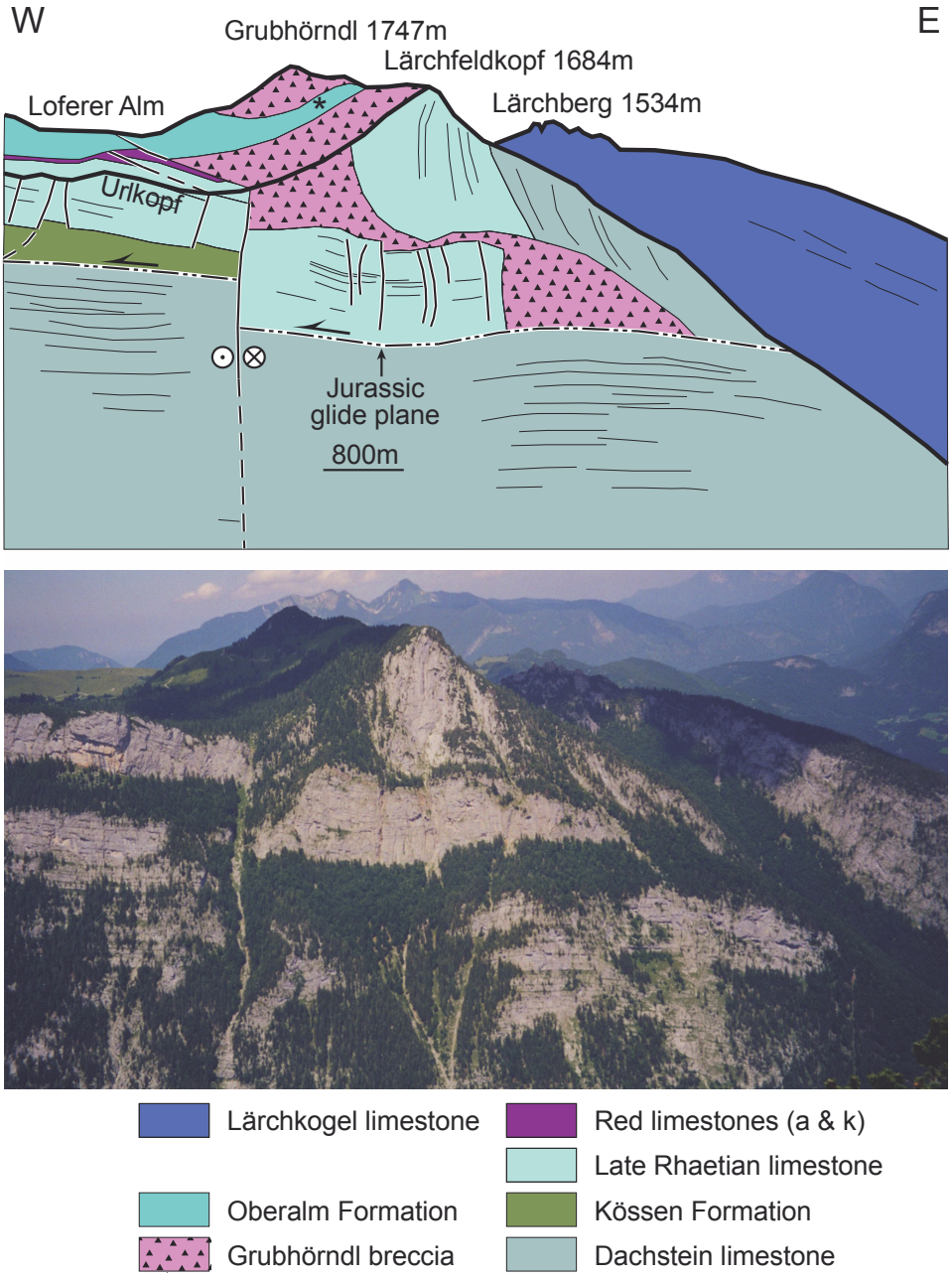

Fig. 8: View of the Loferer Alm and Grubhörndl from the south and its interpretation (adapted from ORTNER et al., 2008). The height of the Lärchfeldkopf olistolithe is at least 350 m. The main problem in emplacement models is the angular relationship between the olistolithe with vertical bedding and the underlying deposits with subhorizontal bedding.

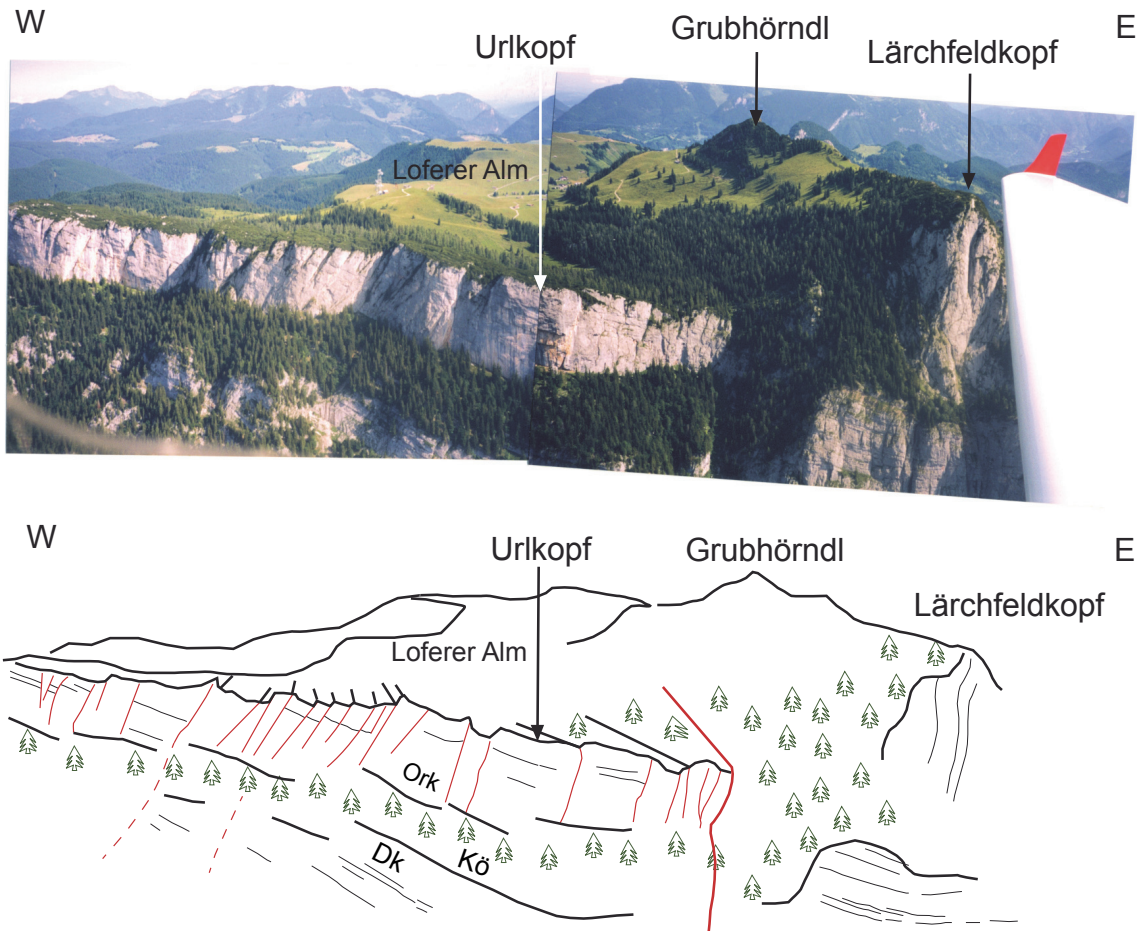

Fig. 9: View of the Sonnenwände from the south. Ork = Upper Rhätian limestone, Kö = Kössen Formation, Dk = Dachstein limestone.

1 Ramp anticline **2 footwall collapse at antithetic normal faults**

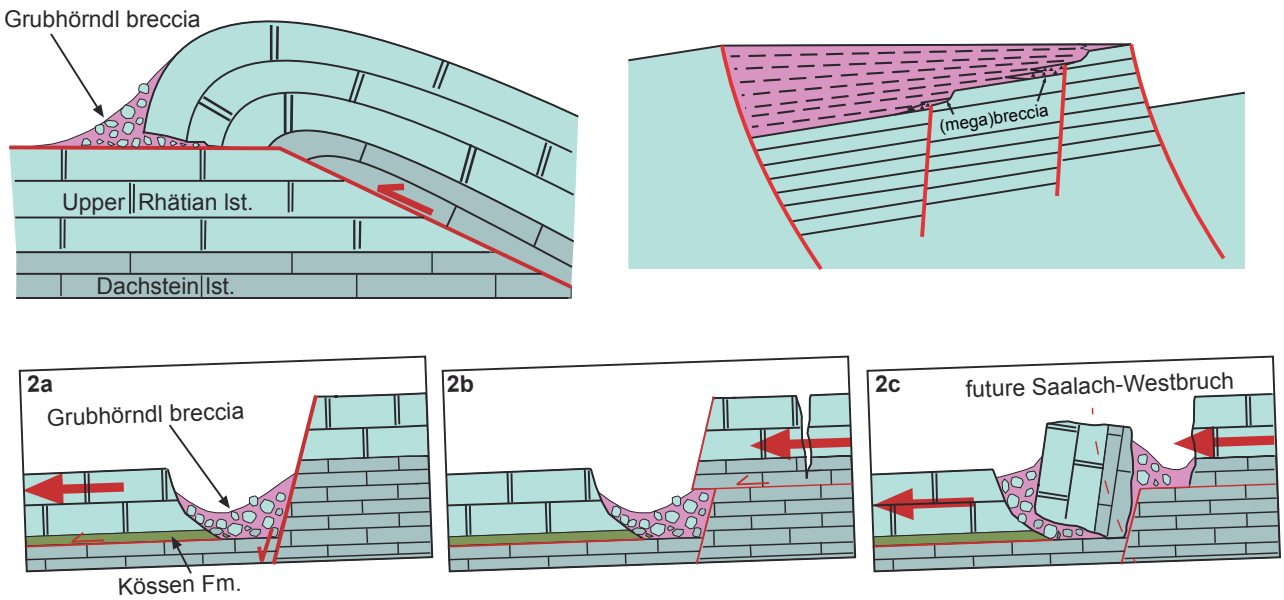

Fig. 10: Emplacement of the Grubhörndl mega-olistolithe by 1 – west-directed thrusting, or 2 – tilting of the succession to the west. Sketches are not to scale. See text for discussion.

It is tempting to interpret the inferred normal fault and roll-over of stop 3 (Fig. 7) together with normal faults decribed here. However, the shallow décollement interpreted there, and the more than 200 m deep décollement in the Kössen Formation preclude a direct connection. Nevertheless, a common driver is probable.

We suggest that the complete sedimentary succession was tilted to the west in the early Late Jurassic (see 2 of Fig. 10 for a sketch). This could have facilitated gliding of the Upper Rhätian limestone, and emplacement of the Grubhörndl megablock. Below and east of the Urlkopf, the Kössen Formation interfingers with the Dachstein limestone, and is already absent below the Lärchfeldkopf (Fig. 8). The end of the Kössen décollement might have detached the Upper Rhätian limestone, thus opening a basin (2a of Fig. 10). A hypotethic antitethic normal fault might have exhumed the top of the Dachstein limestone in the footwall, causing seperation of a huge block and bedding parallel sliding east of the normal fault (2b of Fig. 10). Ongoing westward sliding of the Upper Rhätian limestone west of this fault could have opened more space to progressively tilt the block over the exhumed footwall (2c of Fig. 10). We prefer this interpretation over an interpretation as a ramp anticline (1 of Fig. 10) because (1) a thrust of this dimension should be laterally continuous over several kilometers, (2) thrusting is not compatible with the observation of large scale sliding contemporanous with emplacement of the Grubhörndl block (see above), (3) it would not be possible to redeposit material older than Upper Rhätian limestone, and (4) the base of the block does not show any evidence of thrust related deformation.

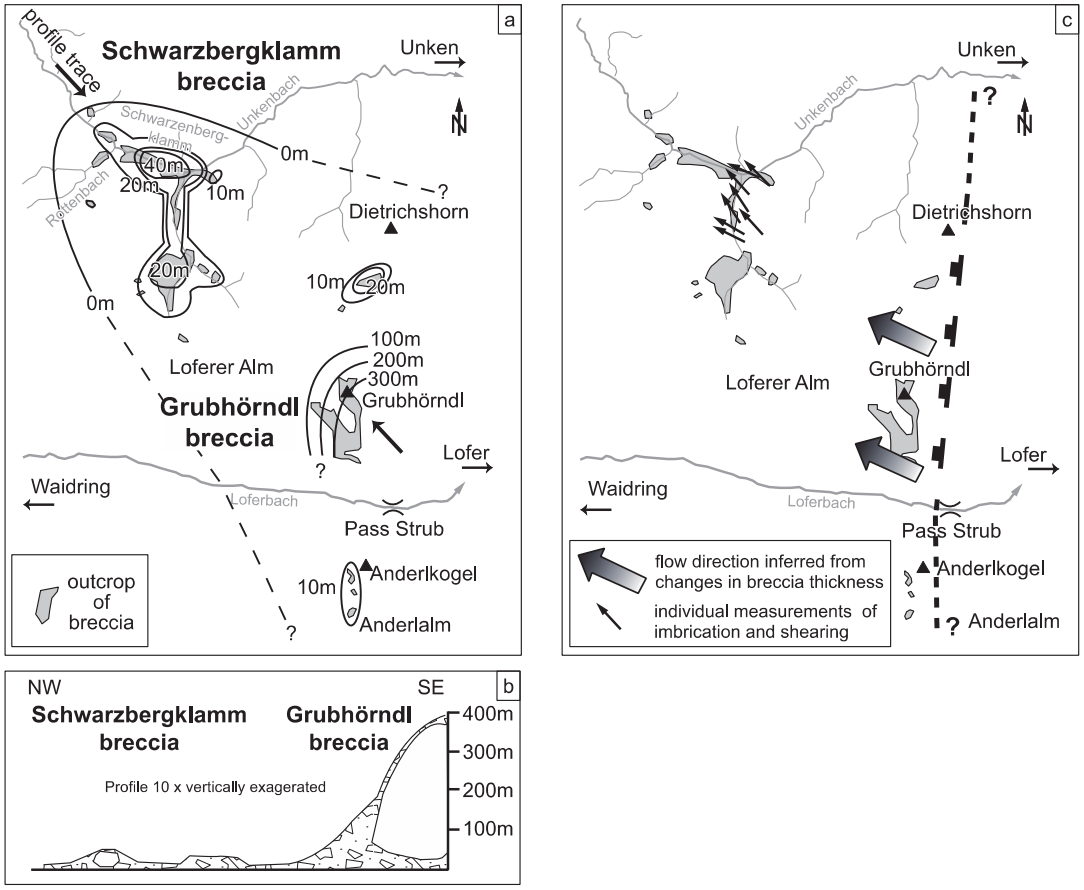

Fig. 11: Thickness distribution of the breccias of the Unken syncline (a, b) and sediment transport directions from imbrication and changes in breccia thickness.

The Grubhörndl block is the only known major Upper Jurassic topographic feature in the area. Most of the block was above the local base level during deposition of the younger part of the Ruhpolding Radiolarite, and the older part of the Oberalm Formation, and a hardground developed on top. The younger part of the Oberalm Formation onlaps the block and the breccia. The delicate hydrozoan fragments found together with other bioclastic material call for a local source. Probably the Grubhörndl olistolithe was originally so big that it had a carbonate platform on its top (ORTNER et al., 2008).

As discussed above, a roughly N-S oriented normal fault is required to facilitate emplacement of the large block. Earlier authors have invoked E-W-striking Jurassic faults to explain the Triassic facies distribution (FISCHER, 1965), Jurassic facies distribution (e.g., PLÖCHINGER, 1953; VECSEI et al., 1989). GAWLICK et al. (1999) suggested Jurassic thrusting at the southern margin of the Osterhorn mountains, and ORTNER (2017a) demonstrated, that thrusting in this area was associated with sinistral wrenching at E-striking faults, using growth strata in the Oberalm Formation Therefore, we suggest that the breccias of the Unken syncline were most probably sourced at the intersection of two perpendicular fault systems (compare CHANNELL et al., 1992), an E-striking being sinistral, and N-striking normal faults. This could explain the NW- to WNW-directed transport and the consistent thinning of the Grubhörndl and Schwarzbergklamm breccias show away from the block (Fig. 11). E-striking sinsitral strike slip faults can probably be interpreted in terms of intracontinental transform faults, linking the opening of the Atlantic ocean with the closure of parts of the Neotethys ocean (SCHMID et al., 2008; SCHMID et al., 2004).

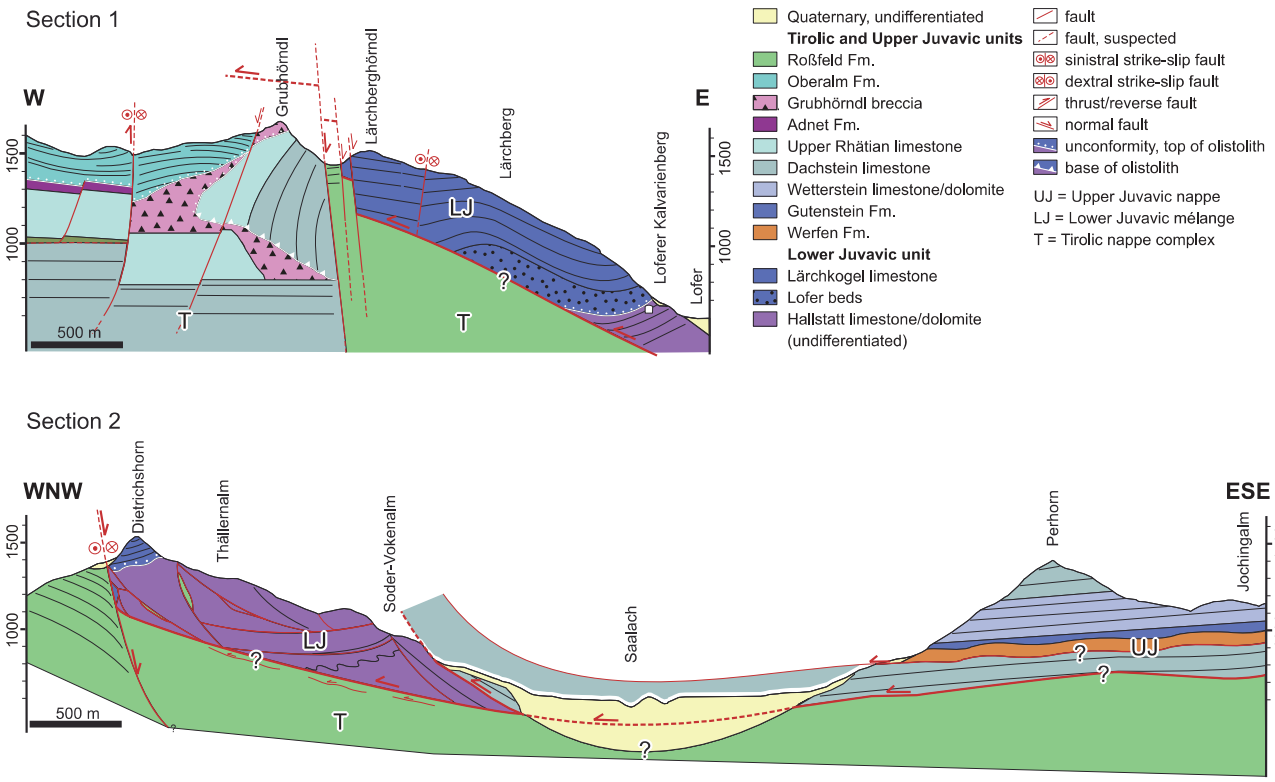

Fig. 12: Cross sections of the Grubhörndl and the Dietrichshorn. Cretaceous nappe boundaries are offset during Miocene faulting. See Fig. 4 for section traces.

Toward the east, the abrupt end of the meadows of the Loferer Alm has geologic reasons, as east and northeast of the Grubhörndl a Miocene fault downthrows the Lower Juvavic against the Tirolic nappe. The view goes across the Gföllhörndl and Lärchberghörndl, in the NE to Dietrichshorn, and below the Saalach valley. These rocky summits are built by the Lerchkogel limestone, which is an Upper Jurassic to Lower Cretaceous carbonate platform, comparable to the Plassen Formation (DARGA & SCHLAGINTWEIT, 1991), unconformably overlying the pelagic limestones and dolomites of the Hallstatt mélange of the Lower Juvavic unit (Figs. 3, 12; LUKESCH, 2003; SANDERS et al., 2007).

An analysis of brittle deformation in the area has shown that six successive paleostress tensors can be distinguished (RITTNER, 2006). These have been interpreted to be related to Cretaceous to Neogene tectonic events, and will be mentioned where appropriate. The normal fault mentioned here has a vertical offset of at least 500 m. Vertical offset diminishes to the north, and sinistral offset increases with the change of fault strike from NNW to N to NE. East of Unken the normal fault is connected to the northernmost branch of the sinistral NE-striking Saalachtal fault. The large-offset normal faulting is related to sinistral transtensive normal faulting during D5 (Fig. 14).

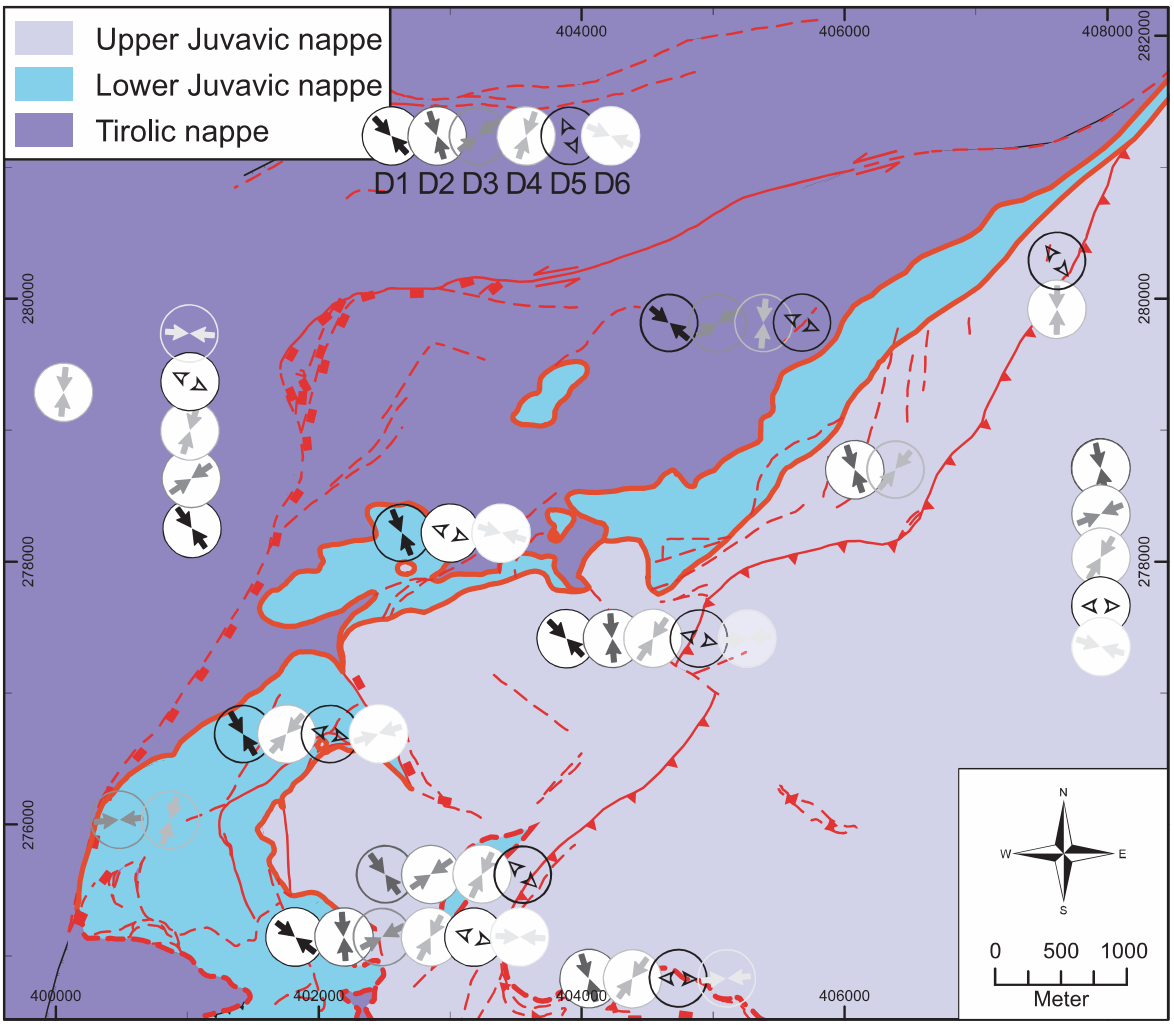

Fig. 13: Measuring stations of brittle faults in the Lofer-Unken area and observed tensors. The point of measurement is given by center of the lowermost symbol, and tensor style can be seen in the example at the top. The stacking pattern of the symbols gives the relative age of the tensors. Open symbols were used for poorly defined tensors. Coordinates: MGI Austria GK M31.

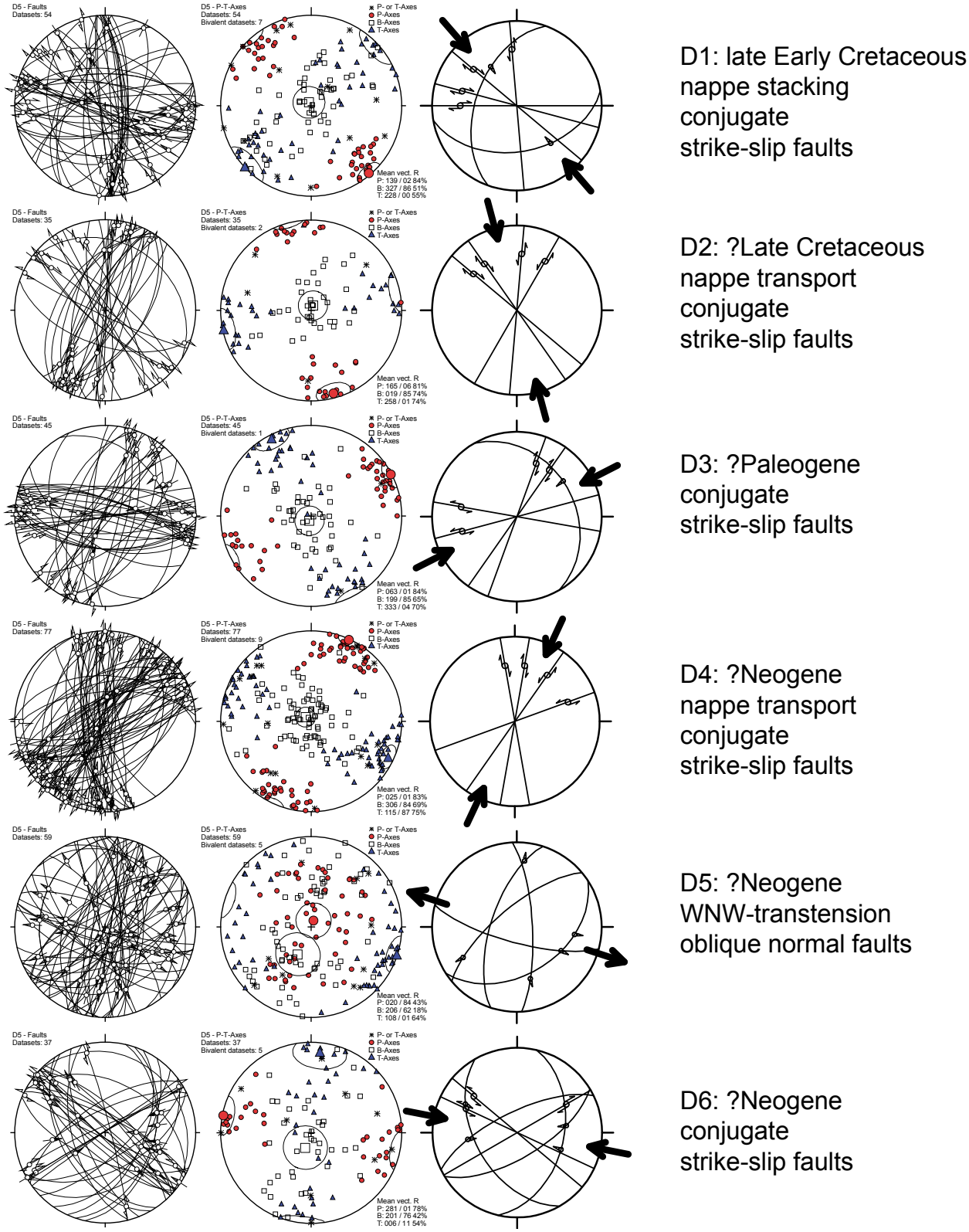

Fig. 14: Brittle faults in the Lofer-Unken area and their tentative interpretation. The diagrams show all faults that have been related to a specific tensor. The left column shows the faults. The middle column gives the P-,T- and B-axes related to the faults, that have been calculated using an angle of 30° between fault plane and P-axis, and the mean vectors of the respective axes with 95% confidence cones. These mean vectors give an estimate of the orientation of the paleostress tensor. The main fault sets observed are shown in the column on the right side.

Stop 8. Loferer Kalvarienberg

Coordinates: E 12.68943, N 47.58576.
Altitude: 650 m.

This stop will demonstrate the Lofer beds and the lowermost part of the Lerchkogel limestone that here discordantly overlies partly dolomitized/silicified Hallstatt limestones (Fig. 15A). The base of the transgressive succession is an interval of clast-supported beachface stylobreccia to conglomerate that consists of clasts of Hallstatt Formation and caliche nodules (Figs. 16A, B). Above, a poorly-exposed backweathering package about 15 m in thickness consists mainly of: (a) medium grey to dark brownish, organic-rich sandy limestones, and (b) organic-rich, brown to blackish marly limestones to marls; both lithologies contain fossils of shallow-marine (and intermittently restricted) environments, such as larger benthic foraminifera (*Anchispirocyclina lusitanica*, *Amijiella amiji*), smaller Textulariina, abundant small gastropods and non-rudist bivalves, and cyanoids. In addition, (c) at least one graded bed ~1 m thick of carbonate-lithic breccia is sharply intercalated; this breccia bed probably had accumulated upon tsunami backflow (Fig. 16C).

In marly limestones of this interval, a large vertebra was found in 2004 by D. Sanders. The vertebra was preparated and lend to the Naturkundemuseum Stuttgart; preliminary inspection by Rainer Schoch suggests that it pertains to a Crocodilian (Fig. 16D). Unfortunately, no further work was done on that vertebra so far. The succession from beachface breccia at the base to organic-rich marls at the top records transgression of a low-energy shore zone over a soil-covered, vegetated land surface that provided input of freshwater as well as of clastic and organic material into a shallow subtidal 'lagoon' seaward of the transgressive fringe (Fig. 15B).

The described interval is overlain by a package ~15 m in thickness of marly to pure limestones with intercalated shell beds of diceratids (*Heterodiceras*) (Fig. 16E). In the shell beds, most of the rudists are embedded toppled and more-or-less fragmented in different stages of taphonomic overprint. The shells are overgrown by other organisms, such as sessile foraminifera, *Milleporidium* (Hydrozoa), serpulids, brachiopods, and *Lithocodium* (Textularina). The co-presence of *Heterodiceras*, *A. lusitanica* and the green alga *Clypeina jurassica* indicates that the Lofer beds here are of latest Tithonian age. Higher up, at Lofer, the lower part of the Lerchkogel Limestone consists of oolithic limestones intercalated with milleporidian biostromes (Fig. 16F). For further details of the described succession it is referred to SANDERS et al. (2007).

Heavy mineral spectra of the Lofer beds are strongly dominated (>50%-99% of total) by apatite, and further characterized by zircon and rutile; tourmaline, staurolite and hornblende are rare. Both the apatite and the zircon show a spectrum of well-rounded to subangular grain shapes. This suggests recycling from pre-existing siliciclastics as well as direct erosion from magmatic rocks. Comparison with literature suggests that the heavy mineral spectrum of the Lofer beds result from a provenance area in which the Alpine Buntsandstein or, more probably, its distal equivalent, the Werfen Formation (Induan-Olenekian), were exposed; in addition, erosion of siliciclastics of the Northern Alpine Raibl beds (Julian-Tuvalian) may have delivered heavy minerals. In the Lofer beds, however, the common presence of subangular apatite with preserved crystal faces requires additional input from erosion of plutonic rocks, consistent with the conclusion derived from the range of grain shapes mentioned before (WOLFGRUBER, 2010).

In the area of Gerhardstein–Hochkranz (Day 2, stops 8-10), the breccias of the Lofer beds contain clasts of mixed siliciclastic-carbonate arenites. These probably were derived from erosion of the Werfen Formation and/or of the Northern Alpine Raibl beds; a derivation from the Alpine Buntsandstein (typically pure quartzites) is considered less probable. A low vitrinite reflectance (0.2-0.5) of coalified plant debris extracted from the Lofer beds indicates peak temperatures of 50-70°C (WOLFGRUBER, 2010).

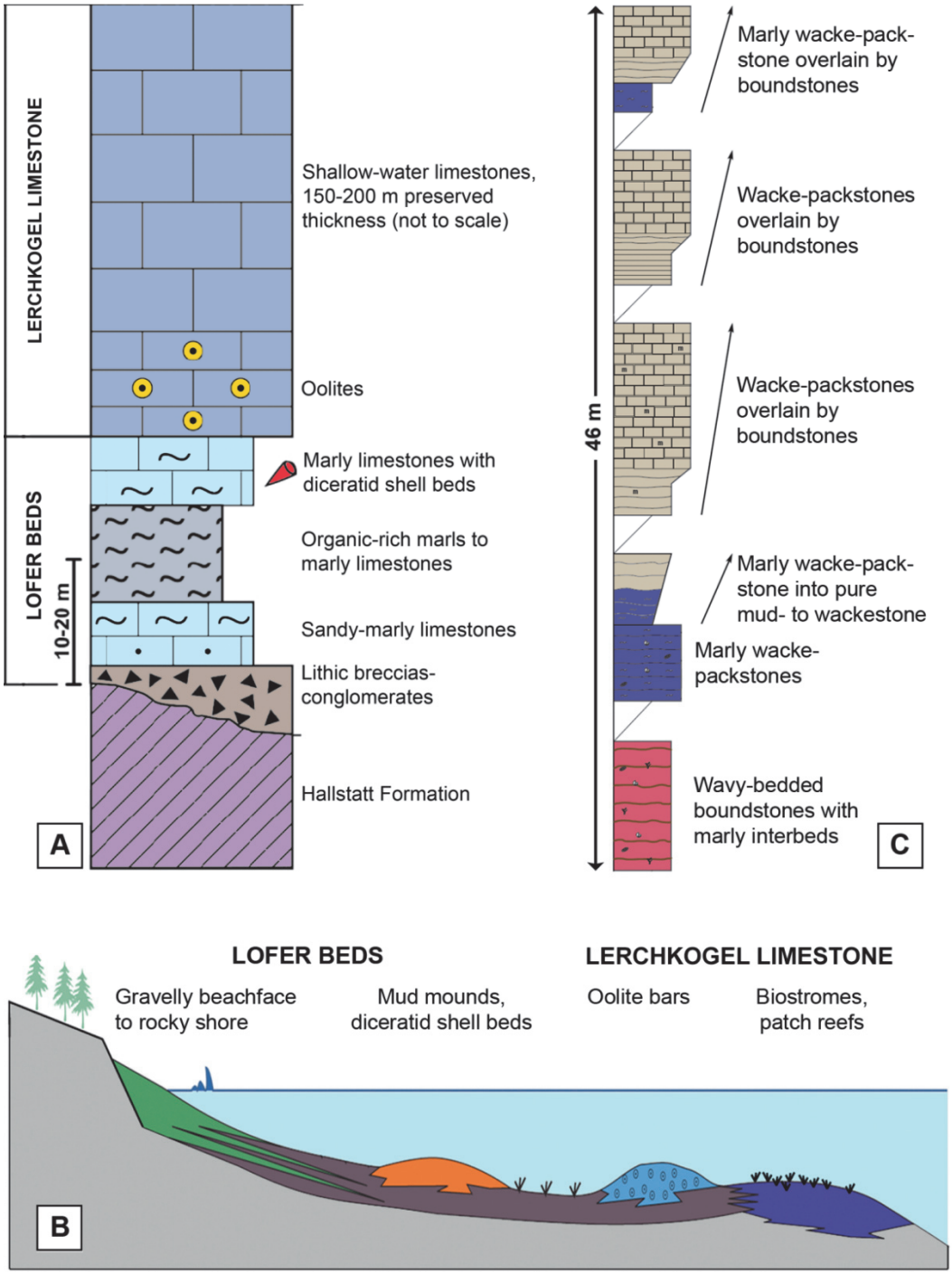

Fig. 15: (A) Generalized section of Lofer beds and Lerchkogel limestone (SANDERS et al., 2007; modified from FERNECK, 1962). (B) Reconstructed transgressive setting (MOSNA, 2010). (C) Upper part of Litzlkogel section, showing a rhythmic packaging of (marly) wacke-packstones and different types of boundstones (MOSNA, 2010).

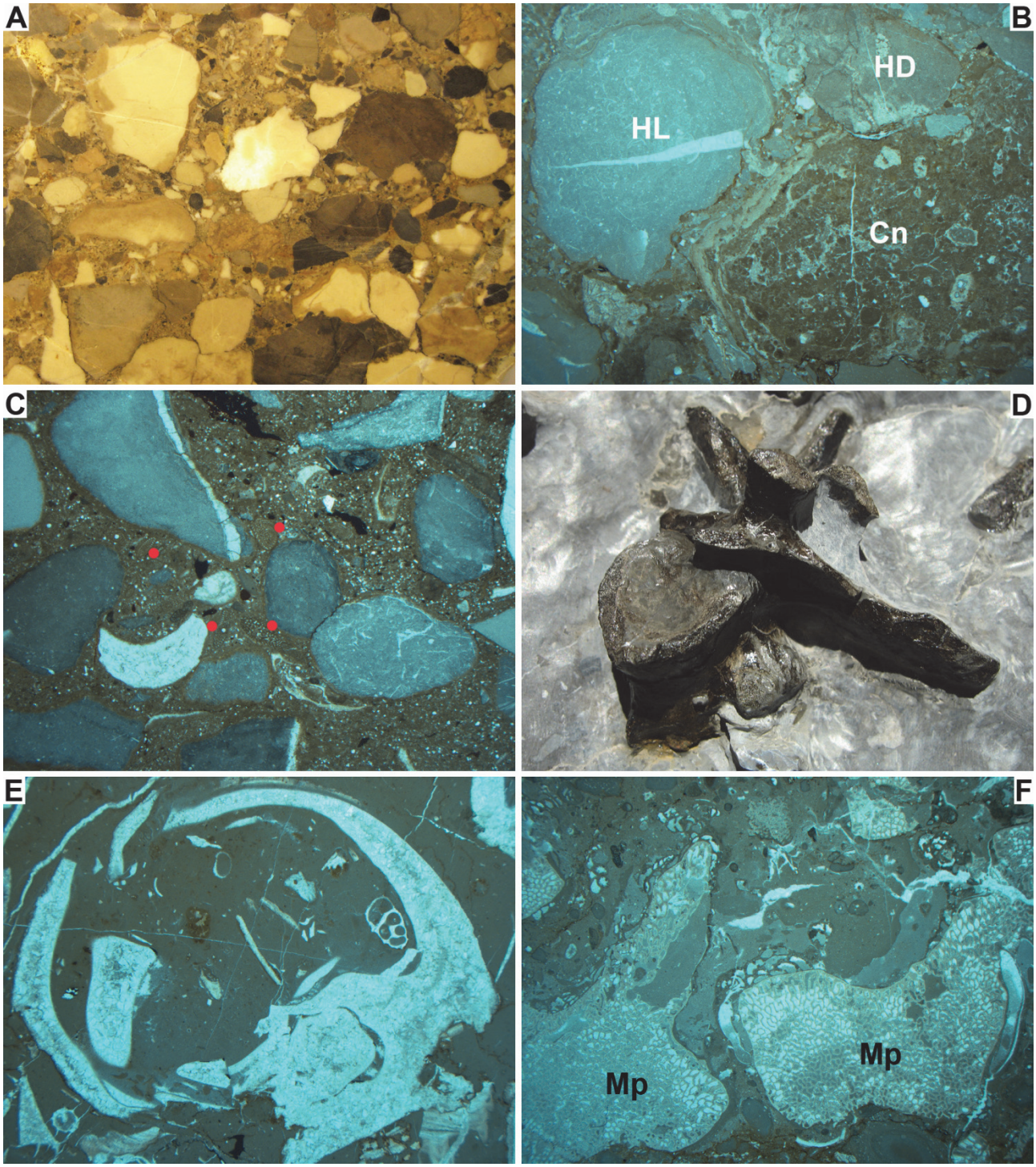

Fig. 16: Lofer beds at Lofer. (A) Polished slab of conglobreccia at the base of the Jurassic section. Width: 10 cm. (B) Basal breccia: Clasts of Hallstatt Limestone and -dolomite (HL, HD), and a caliche nodule (Cn). Width: 29 mm. (C) Event bed (probable tsunamite): Clasts of Hallstatt Formation and plant debris in a matrix of bioclastic wackestone with Anchispirocyclina lusitanica (red dots). Width: 22 mm. (D) Reptile vertebra, probably from a Crocodilian, in marly limestones of the Lofer section. Width: ~10 cm. (E) Diceratid rudist from a shell bed. Width: 22 mm. (F) Milleporidium (Mp), overgrown by sessile foraminifera. Width: 29 mm.

Day 2 – Weißbach area: Stops 9 to 14

Southeast of Lofer, the Gerhardstein and Hochkranz klippen of the Lower Juvavic nappe sit on top of a lower Cretaceous synorogenic sedimentary succession (Schrambach and Roßfeld Formations) of the Tirolic nappe complex. The Lerchkogel limestone cliffs of the klippen are widely visible. According to HAHN (1913a), the Gerhardstein has the best exposures of a thrust in the Alps of the state of Salzburg („*die schönsten Überschiebungsaufschlüsse, die in den gesamten Salzburger Alpen zu sehen sind*"), and we showcase one these outcrops at stop 9.

Locally, the transgression of the Lerchkogel limestone directly onto Hallstatt dolomite is mappable (Fig. 17), however, in other places, the Lofer beds are found at the base of the klippen. This suggests that the Late Jurassic „neoautochthonous" (e.g., MANDL, 2000) succession covered a preexisting topography, and was detached and transported together with the underlying Hallstatt dolomites.

In contrast to the Unken syncline, the Lower and Middle Jurassic of the Tirolic unit is developed in basinal facies. Red limestones of the Adnet Formation are directly overlain by the Allgäu Formation, and the Ruhpolding radiolarite (Fig. 3). We will study this succession at stop 13. Within the Red limestones, huge slide blocks and associated breccias are present (KRAINER et al., 1994). Stop 12 shows the base of such a slide block, deformation at its base and the underlying red limestones.

Stop 9. Base of Gerhardstein Klippe south of Gerhardstein

Coordinates: E 12.75830, N 47.53468.
Altitude: 1250 m.

We follow a dirt road from Stocklaus toward Gerhardstein, passing the Wandbauer hamlet. At stop 9, the basal thrust of the Gerhardstein klippe is exposed in an outcrop along a new dirt road. The footwall are not the Schrambach or Roßfeld Formations of the Tirolic unit, but a slice of the Tirolic unit that has been emplaced on top of another slice of the Lower Juvuvic nappe out-of-sequence. Such slices are common at the base of the klippen east of Weißbach, and the largest one is found south of the Hochkranz (SIEWERT, 1973). Most of these slices are part of the Oberalm Formation, only the one at stop 9 has an internal succession of Oberalm Formation, Ruhpolding radiolarite and Schrambach Formation, which is emplaced onto a tectonically deeper slice of Lerchkogel limestone. The outcrop sketches of Figures 18g and h are from the base of this slice, a few tens of meters below stop 9.

The tectonic contact is characterized by penetrative shear bands in the Schrambach marls, and duplexing in the more competent Ruhpolding radiolarites and Oberalm limestones. The contact shows open wavy folding, and the deepest parts being affected by renewed thrusting parallel to foliation that brings the Schrambach marls on top of the Lerchkogel limestone (described as „Verkeilung" by JACOBSHAGEN & KOCH, 1959). This gives a model for the emplacement of the deepest slice below stop 9.

Local transport directions based on shear band geometry is top to NNE. However, analysis of a larger number of shear bands at the base of the lowermost slice (outcrops a and b of Fig. 18). results in north-directed tectonic transport. Taking into account all measured data from the base of the Gerhardstein and Hochkranz klippen (MOSNA, 2010; WOLFGRUBER, 2010), transport directions vary from top to NW to top to NE. This is in accordance with the observed tensors D1 to D3 of Figures 13 and 14 deduced from the analysis of brittle fault planes. We speculate here that this succession of tensors implies that transport on out-of-sequence thrusts changes progressively from top NW to top NE from base to top as new slices form.

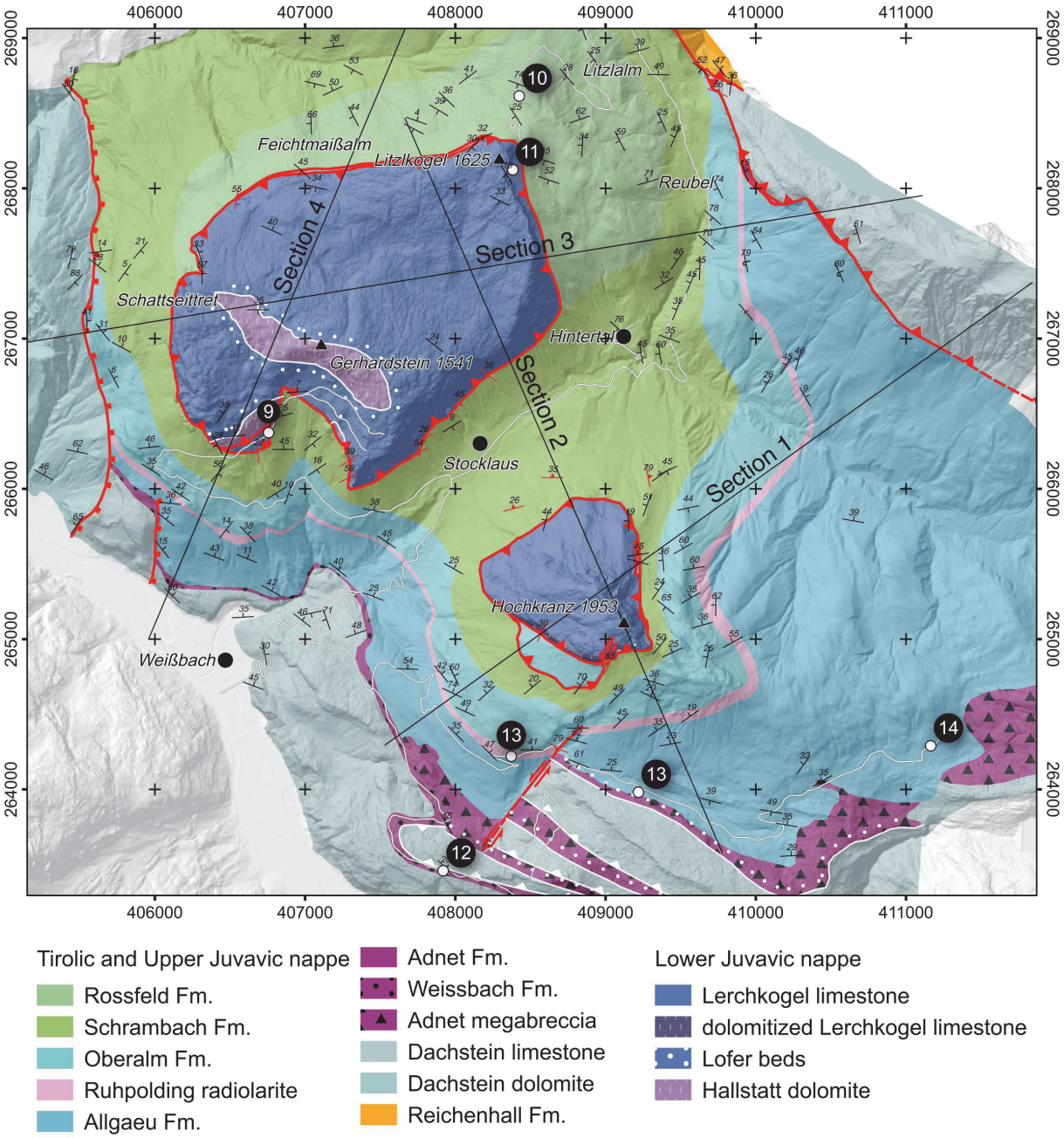

Fig. 17: Tectonic map western end of the Juvavic nappe complex in the Weißbach area, compiled from MOSNA (2010) and WOLFGRUBER (2010). Minor changes according to SIEWERT (1973) and PAVLIK (2006). SSE part redrawn from KRAINER et al. (1994). Numbers 9 – 14 indicate field trip stops of day 2. Sections are shown in Figure 20. Coordinates: MGI Austria GK M31.

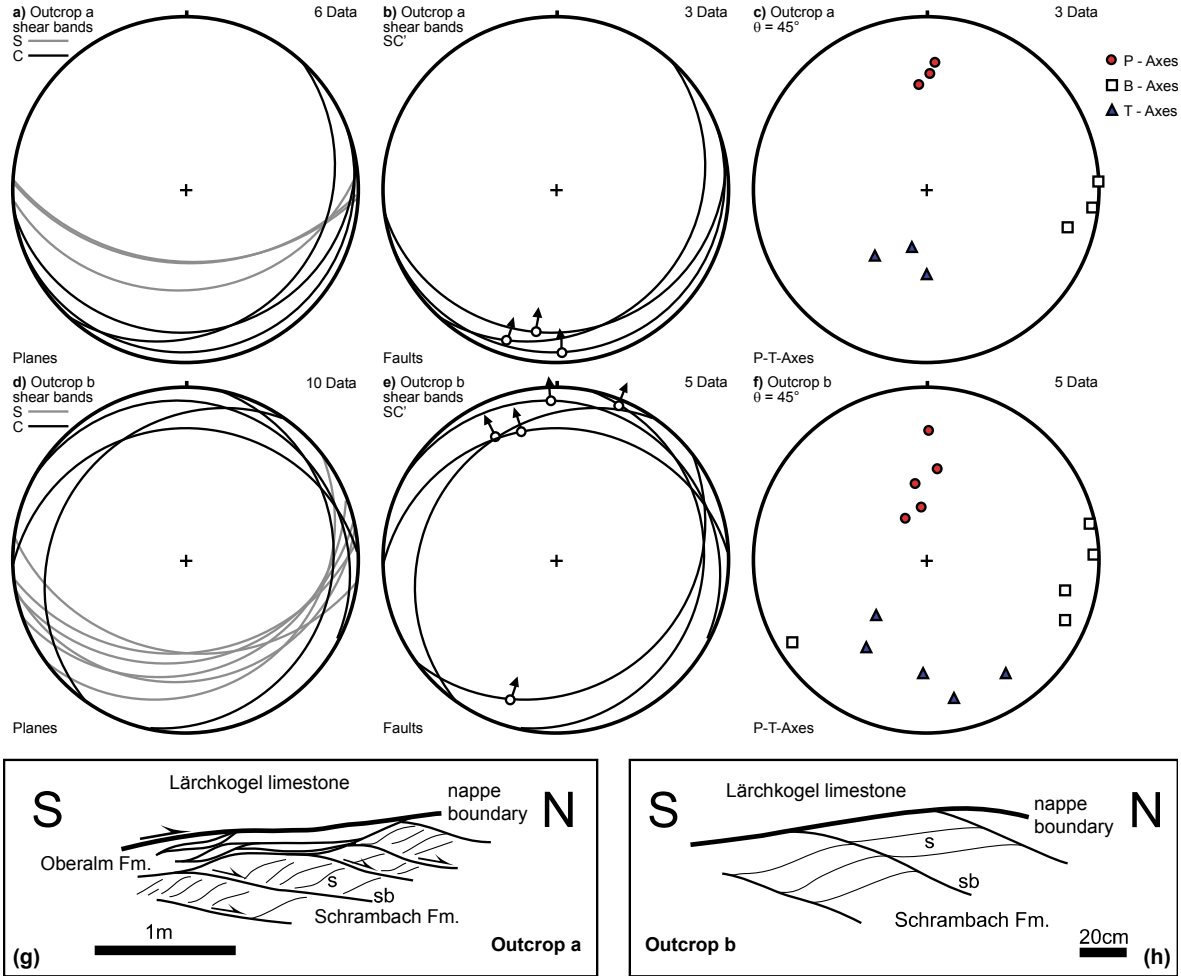

Fig. 18: Structural data from two outcrops at the base of the Gerhardstein klippe in the immediate vicinity of stop 9. Shear bands in Schrambach marls were used to deduce transport directions. a, d) Great circles of s- and c-planes; b, e) Hanging wall movement on C-planes calculated from pairs of S- and C-planes; c, f) Kinematic axes derived from movement on C-planes, using an angle of 45° between C-plane and P-axis. g, h) Sketches of structures at the two outcrops. Note slice of Oberalm Formation between Schrambach Formation of the footwall and Lerchkogel limestone of the hanging wall in (g).

Stop 10. Olistolithe within the Roßfeld Formation at Litzlalm

Coordinates: E 12.77994, N 47.55492.
Altitude: 1420 m.

We go back to Stocklaus, pass the Hirschbichl saddle, continue past the Litzlalm toward Litzlkogel. South of the road to stop 10, olistoliths a few tens of meters in size of limestones are visible that are intercalated into the Rossfeld Formation. These olistoliths will not be visited. They are briefly characterized as cherty spiculitic wacke-packstones with a few inoceramid fragments, small planktic foraminifera and a few grains of quartz, glauconite and phosphorite. The co-presence of small planktic foraminifera with inoceramid fragments suggests that the spiculites accumulated somewhen during the latest Jurassic to early Cretaceous (MOSNA, 2010).

The olistolith that is seen with the excursion was studied along a section 14 m in length. The lower part (2 m) consists of strongly stylolitized, red-coloured lime mudstones to wackestones with radiolarians; this lithology was interpreted as Hallstatt Limestone. The middle part (2 m) contains red to brown

arenites (grainstone and packstone texture) mainly of crinoid ossicles and a few small fragments of rudists and non-rudist bivalves, bryozoans and skeletal sponges. The former matrix of lime mud is selectively replaced by chert, and the interstitial pore space in grainstone texture is filled with megaquartz cement.

The upper 10 m of the section consists of grey wackestones with bioclasts of deep-water and neritic habitats, respectively. Aside of crinoid ossicles, the deep-water bioclastic fraction is characterized by rare globotruncanids (cf. *Rotalipora*; Albian *p.p.* to Cenomanian), lagenids (*Nodosaria*, *Lenticulina*) and Textulariina; the neritic fraction comprises bioclasts of bryozoans, brachiopods and corals. Notably, also calpionellids and a few clasts of shallow-water limestones (e.g., bioclastic grainstones) were identified in the matrix. The co-presence of cf. *Rotalipora* with calpionellids (up to Valanginian) indicates substantial reworking – as supported also by the clasts of shallow-water limestones – and a sediment record up to at least the middle to upper Albian (maximum: Cenomanian, because of total range of *Rotalipora*) (MOSNA, 2010).

Stop 11. Lofer beds at base of Gerhardstein klippe, and Lerchkogel limestone at Litzlkogel

Coordinates: E 12.77970, N 47.55053.
Altitude: 650 m.

We continue on the dirt broad to a small saddle at 1460 m, and follow the footpath toward Litzkogel (165 m elevation difference). At 1500 m, we pass a preliminary section (Fig. 15C) through the upper part of the exposed succession displays a vertical packaging between: (a) backweathering, more-or-less marly, bedded wacke- to packstones (Fig. 19A) that grade up-section into (b) outweathering, thick-bedded to unbedded intervals with boundstones. The wacke-packstones are rich in smaller benthic foraminifera, peloids, fragments of dasycladalean algae and of corals, echinoderm ossicles (e.g., echinoid spines), brachiopods, *Tubiphytes* and, in a few intervals, coalified plant debris. The boundstones, in turn, contain dendroid corals and *Milleporidium* (Figs. 19B, C) that may show complex encrustation successions. The matrix of these boundstones contains fragments of diverse dasycladaleans, benthic foraminifera and serpulids; locally, boundstones of 'Porostromates' of type *Cayeuxia*, and discrete masses of microbialites are present (Figs. 19D, E, F).

The significance of the rhythmic packaging between wacke-packstones and boundstones is not fully clear as yet. If the wacke-packstones represent a bathymetrically deeper facies than the boundstones, at least the upper three packages may represent upward-shoaling/cleaning cycles. In the lower part of the section, however, input of siliciclastic sediment took place also during boundstone accumulation. More detailed sampling were required to better resolve bathymetric trends and patterns of siliciclastic input associated with sediment packaging.

The summit of Litzlkogel offers a wide view of the surrounding mountains. In the east, an open, NW plunging anticline is seen in the cliffs below the Kammerlinghorn summit (Hundstod anticline; TOLLMANN, 1969). In map view, the trace of the axial plane of this anticline is parallel to the trace of the syncline of the Weißbach syncline. The Gerhardstein and Hochkranz klippen are in the western limb of this syncline. The summits in the north are in the Middle Triassic Ramsau dolomite of the Upper Juvavic nappe. In the valley east of the Hirschbichl saddle the Tirolic nappe complex disappears below the Upper Juvavic unit, and all units dip to NW. This northwesterly dip is also seen in the section 2 of Figure 20 below the Hochkranz klippe, that we see south of Litzlkogel, and is a regional feature. The Weißbach syncline and the adjacent NW-plunging Hundstod anticline seem to be a local feature that

is oblique to most of the structures of the Northern Calcareous Alps. The Weißbach syncline is parallel to the Hundstod thrust ("Hundstod-Aufschuppung"; BARTH, 1968; HAHN, 1913a; TOLLMANN, 1969, 1976b), and may be interpreted on terms of drag along the fault, thus not related to regional folding event.

The Hintertal syncline has a very open monoclinal geometry (section 2 of Fig. 20), while the Weißbach synline has a tighter hinge zone in directly adjacent to the Hundstod thrust. The overprint of two generations of folds with perpendicular fold axis leads to a Type 1 fold interference pattern (Fig. 21). Because of the monoclinal shape of the Hintertal syncline the elongate basin is open to the NW and SW, and is comparable to a quarter bathtub.

Stop 12. Base of a slide block in Early Jurassic sediments (Weißbach Formation)

Coordinates: E 12.77402, N 47.50857.
Altitude: 1100 m.

We return from Litzlkogel to Pürzlbach, and follow the dirt road from Pürzlbach toward Kopfstein. After crossing the Brechlbach creek, the road follows a layer of incompetent rock between Dachstein limestone (Fig. 17).

These rocks are red bedded limestones that are a local equivalent of the Adnet Formation of the Red limestones, and have been defined as Weißbach Formation (KRAINER et al., 1994; MOSTLER & KRAINER, 1993). These limestones were deposited on a slope, and contain breccia beds. On top of the Weißbach Formation, the base of a Dachstein slide block is exposed. The sediment is seen to be ploughed by the block during roughly N- to NW-directed movement (KRAINER et al., 1994 and own data). The slide block is overlain by alternating breccias and megabreccias of the Adnet Formation and two Dachstein slide blocks (Fig. 17). The capping sequence of the megabreccias ends with mangenese rich laminated marls of Toarcian age of the younger Allgäu Formation (KRAINER et al., 1994). Laterally, this breccia succession is replaced by the Allgäu Formation (Figs. 3, 17).

Stop 13. Basinal sedimentary succession from Early to Late Jurassic, soft-sediment deformation in Upper Jurassic

Coordinates: E 12.77992, N 47.51542 and E 12.79117, N 47.51333.(two substops, see text)
Altitude: 1200 m.

We return to Pürzlbach and follow the dirt road toward the Kallbrunnalm. Between 1160 and 1250 m the sedimentary succession from the Allgäu Formation into the Ruhpolding radiolarite and Oberalm Formation is exposed. The Allgäu Formation includes bioturbated cherty limestones and marls („Fleckenkalke und Fleckenmergel“), shales rich in manganese and cm-bedded siliceous limestones to cherts (KRAINER et al., 1994). The dirt road exposes the uppermost part of the succession, starting with the thin-bedded siliceous limestones and cherts, that can be compared to the Chiemgau beds of Middle Jurassic age (TOLLMANN, 1976a). Cm- to dm-bedded cherts of the Ruhpolding radiolarite follow on top, and then micritic limestones of the Oberalm Formation A set of NE-dipping normal to oblique normal faults crosscuts the Oberalm Formation, and some of the faults are sealed within the Oberalm Formation (Fig. 22).

Where the dirt road crosses the Brechlbach, a NE-striking fault separates the Oberalm Formation on the NW side from the Allgäu Formation on the SE side. There, the succession on top of the olistolithes starts with a few meters of grey to red limestones, followed by mangenese ore and then maganese-rich marls (KRAINER et al., 1994). The geologic map (Fig. 17) shows that the fault delimits the stack of

olistolithes, but does not cut across the lowermost block. This suggests that fault activity was initially related to olistolithe emplacement and persisted into the Late Jurassic. Initially, the Allgäu Formation covered submarine topography, while the stack of olistolithes was still mobile. Glide processes may have evacuated the olistolithes NW of the fault.

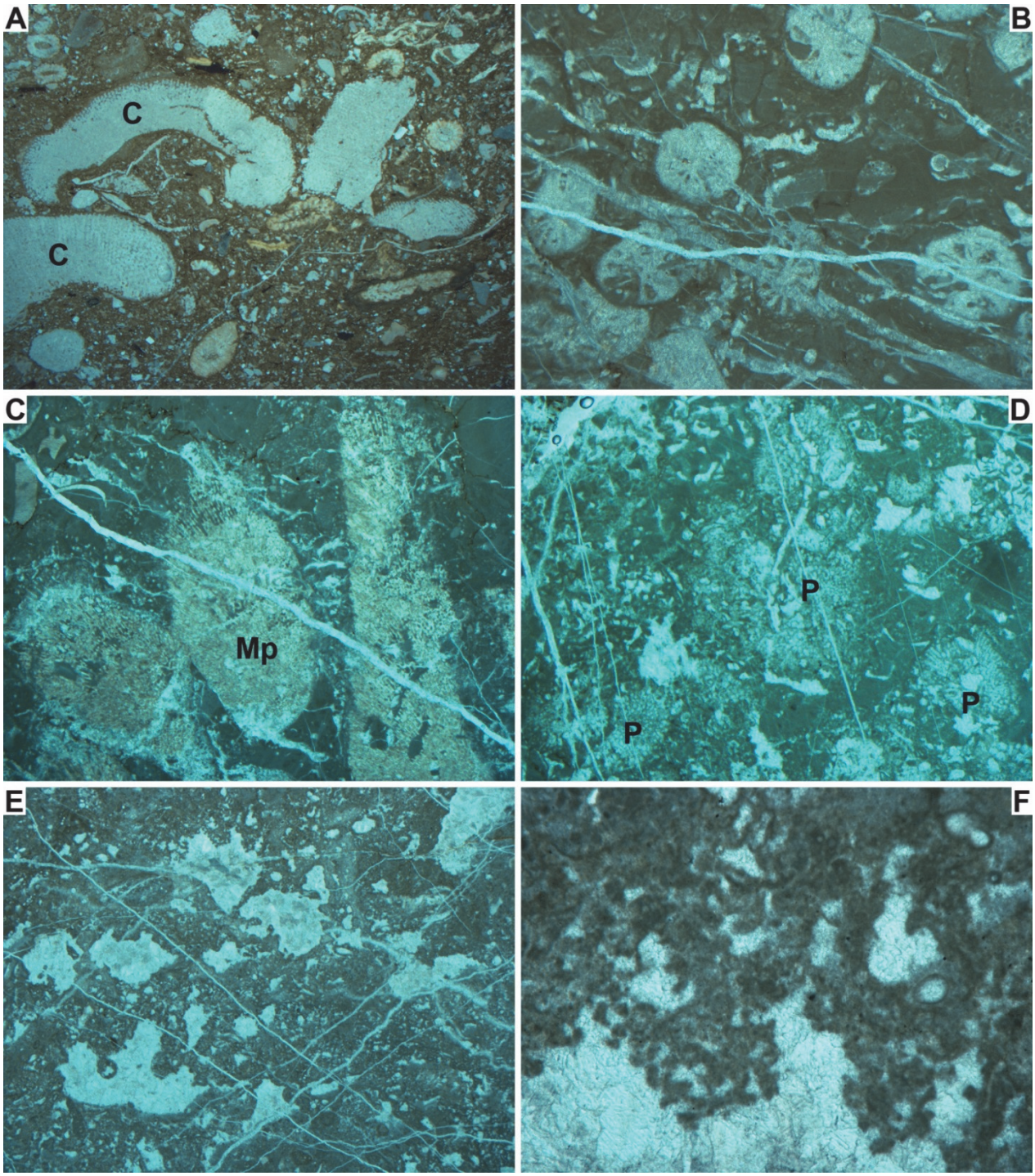

Fig. 19: Litzlkogel section. (A) Brown, marly bioclastic packstone with coral fragments (C). Width: 22 mm. (B) Floatstone with dendroid coral. Width: 29 mm. (C) Boundstone with branched Milleporidium (Mp). Width: 17.5 mm. (D) Porostromate-microbialite boundstone. Width: 8.5 mm. (E) Fenestral microbialite mainly with thrombolithic fabric. Width: 14 mm. (F) Detail of thrombolithic fabric. Width: 2.2 mm.

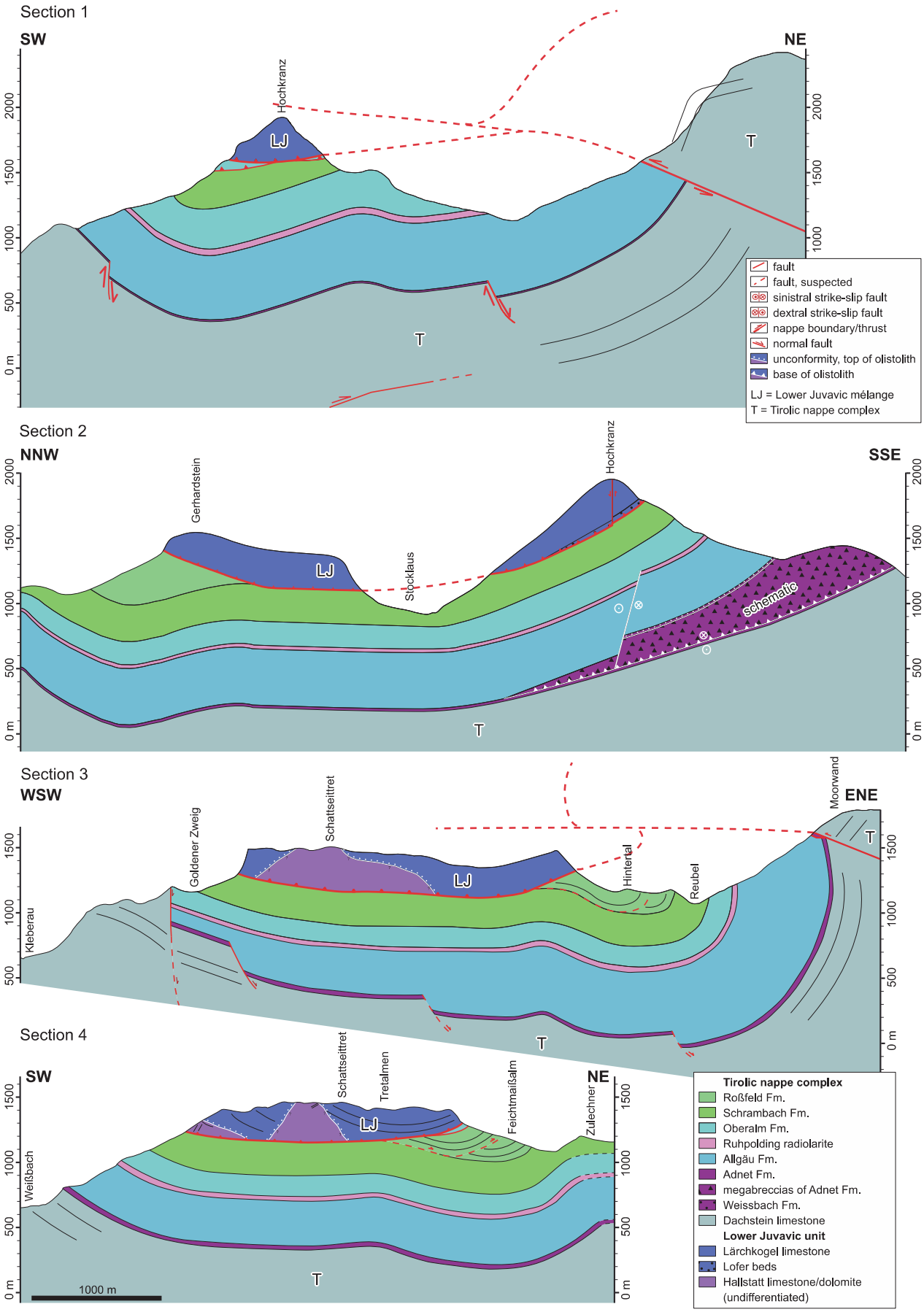

Fig. 20: Cross sections of the Gerhardstein and Hochkranz klippen. See Figure 17 for section traces.

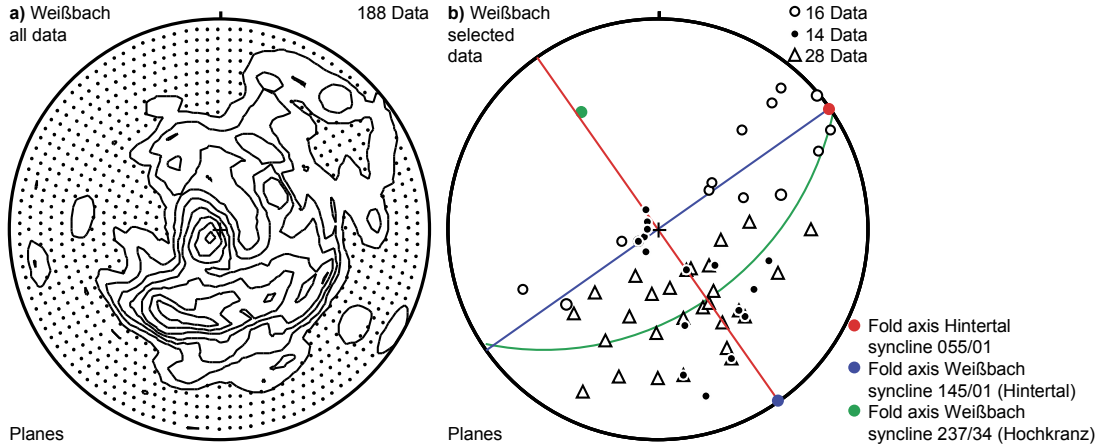

Fig. 21: Analysis of Bedding orientations in the Weißbach area (see Fig. 17). a) Contour plot of all bedding planes of the Weißbach area. There is no straightforward interpretation of the observed distribution of bedding poles. b) Separating data east of Hintertal and Reubel (Fig. 17) allows to calculate a horizontal axis for the Weißbach syncline (poles to bedding shown by open circles and fille blue circle for fold axis). Open triangles indicate bedding poles around Hochkranz, giving a NW-plunging fold axis (filled green circle) for the Weißbach syncline. Bedding orientations selected along the trace of section 2 (black filled circles) allow to calculate an NE-trending axis for the Hintertal syncline.

Where the dirt road crosses the Brechlbach, a NE-striking fault separates the Oberalm Formation on the NW side from the Allgäu Formation on the SE side. There, the succession on top of the olistolithes starts with a few meters of grey to red limestones, followed by mangenese ore and then maganese-rich marls (KRAINER et al., 1994). The geologic map (Fig. 17) shows that the fault delimits the stack of olistolithes, but does not cut across the lowermost block. This suggests that fault activity was initially related to olistolithe emplacement and persisted into the Late Jurassic. Initially, the Allgäu Formation covered submarine topography, while the stack of olistolithes was still mobile. Glide processes may have evacuated the olistolithes NW of the fault.

The differences in thickness and facies in the Lower Jurassic sediments have been interpreted in terms Early Jurassic transtensive basin formation (CHANNELL et al., 1992; KRAINER et al., 1994), which is supported by the synsedimentary faults in the Oberalm Formation, given that the same fault system remained active into the Late Jurassic.

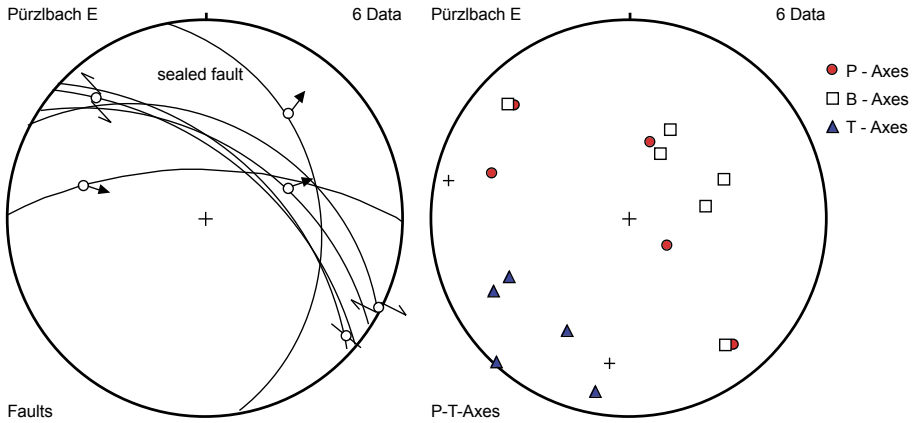

Fig. 22: Faults in the Oberalm Formation at stop 13, that are probably syndepositional. The girdle distribution of P- and B- axes indicates transtension.

Stop 14. View of the Kammerlinghorn from Kallbrunnalm

Coordinates: E 12.81699, N 47.51622.
Altitude: 1450 m.

This stop is a second alternative to stop 11 at the summit of Litzlkogel in case of poor weather conditions.

Concluding remarks

This field trip has shown some key events in the evolution of the NCA:

1) Early Jurassic basin formation and associated differentation of facies and emplacement of huge olistolithes, related to opening of the Central Atlantic.
2) Late Jurassic deposition of large breccia bodies and olistolithes. In the Late Jurassic, facies differences are observed between the Tirolic and Lower Juvavic units. Continental to shallow marine deposits are found on top of the Lower Juvavic unit, while allodapic limestones interclated with pelagic deposits are found on top of the Tirolic unit. However, this event is partly contemporaneous with emplacement of the sedimentary mélange of the Lower Juvavic units into pelagic sediments by glide processes (Fig. 1), and by transpression at the Trattberg rise east of the field trip area (see discussion above, Stop 7). Cross sections in the Salzkammergut area 100 km east of Lofer show very open folds onlapped and sealed by Upper Jurassic sediments (MANDL, 2013), and PICOTTI & COBIANCHI (2017) discussed lithospheric folding to explain thickness differences in Upper Jurassic sedimentary successions of the easternmost Southern Alps. Whatever type of tectonic activity it was, it did cause uplift and erosion in some areas, und subsidence in other areas. The uplifted areas were those affected by erosion and retransgression during the Late Jurassic, and those documented all across the Middle and Eastern NCA (e.g., Loferer beds, Oberalmer Basiskonglomerat, Obersee breccia (e.g., LEIN et al., 2009; PLÖCHINGER, 1953; SANDERS et al., 2007)
3) Inversion of the continental margin starting at the end of the Early Cretaceous. During this event, the nappes of the NCA formed (d1 to d4 of Fig. 23). Part of the Lower Juvavic unit, and the Upper Juvavic nappe, were detached and emplaced onto Early Cretaceous synorogenic deposits. Consequently, the Lower Juvavic unit is either „in place“ (i.e., not transported during Lower Cretaceous shortening; in the surrounding of Kuchl in Fig. 1), or it is a nappe (N and SW of Lofer in Fig. 1; see also SCHWEIGL & NEUBAUER, 1997). Transport of the Lower Juvavic nappe was most probably together the Upper Juvavic nappe (G. Mandl in SCHEIDLEDER et al., 2001).
4) Cenozoic faulting controls much of the present-day morphology of the NCA. Two dominant processes interact: lateral escape of crustal blocks that affects mainly the internal part of the Eastern Alps, and only the southernmost part of the central NCA (RATSCHBACHER et al., 1991), and postcollisional oblique convergence between the Eastern Alps and the European foreland. The latter causes NE-striking sinistral tear faults rooting at the base of the Subalpine Molasse and/or Helvetic nappes (ORTNER et al., 2015). As lateral escape is increasingly extensional toward the east, these tear faults, i.e. the Saalachtal fault, end in an extensional horse-tail splay toward the south and sinistral offset does not reach the southern margin of the NCA (d5 of Fig. 23).

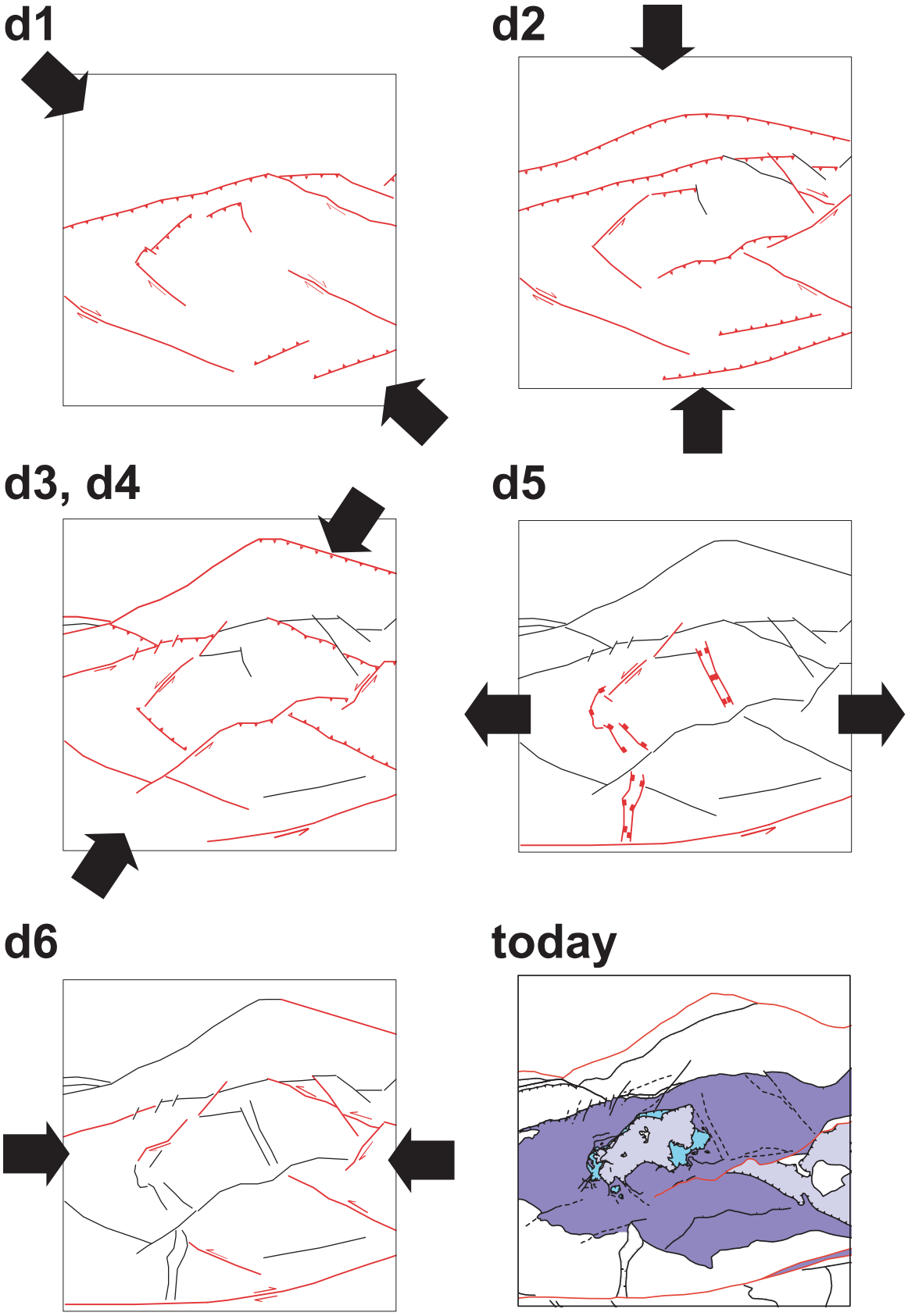

Fig. 23: Attempt to correlate the paleostress tensors of Figures 13 and 14 to the activity of individual faults observed in the field trip area (modified from RITTNER, 2006). Coloring of tectonic units as in Fig. 1.

References

AMPFERER, O. (1927): Über den Westrand der Berchtesgadener Decke.- Jahrbuch der Geologischen Bundesanstalt, 77, 205 - 232, Wien.

BARTH, W. (1968): Die Geologie der Hochkalter-Gruppe in den Berchtesgadener Alpen.- Neues Jahrbuch für Geologie und Paläontologie, Abhandlungen, 131, 119-177, Stuttgart.

BRAUNSTINGL, R. (2005): Geologische Karte von Salzburg 1:200.000.- Geologische Bundesanstalt, Wien.

CHANNELL, J. E. T., BRANDNER, R., SPIELER, A. & STONER, J. S. (1992): Paleomagnetism and paleogeography of the Northern Calcareous Alps (Austria).- Tectonics, 11, 792 - 810, Washington, D.C.

DARGA, R. & SCHLAGINTWEIT, F. (1991): Mikrofazies, Paläontologie und Stratigraphie der Lerchkogelkalke (Tithon-Berrias) des Dietrichshorns (Salzburger Land, Nördliche Kalkalpen).- Jahrbuch der Geologischen Bundesanstalt, 134, 205-226,

DARGA, R. & WEIDICH, K. F. (1986): Die Lackbachschichten, eine klastische Unterkreide-Serie in der Unkener Mulde (Nördliche Kalkalpen, Tirolikum).- Mitteilungen der Bayerischen Staatssammlung für Paläontologie und historische Geologie, 26, 93-112, München.

DECKER, K., FAUPL, P. & MÜLLER, A. (1987): Synorogenic sedimentation in the Northern Calcareous Alps during the Early Cretaceous.- In: FAUPL, P. & FLÜGEL, H. W. (Eds.), Geodynamics of the Eastern Alps, 126 - 141, Wien (Deuticke).

DECKER, K., PERESSON, H. & FAUPL, P. (1994): Die miozäne Tektonik der östlichen Kalkalpen: Kinematik, Paläospannungen und Deformationsaufteilung während der "lateralen Extrusion" der Zentralalpen.- Jahrbuch der Geologischen Bundesanstalt, 137, 5-18, Wien.

DIERSCHE, V. (1980): Die Radiolarite des Oberjura im Mittelabschnitt der Nördlichen Kalkalpen.- Geotektonische Forschungen, 58, 217 S., Stuttgart.

FERNECK, F. A. (1962): Stratigraphie und Fazies im Gebiet der mittleren Saalach und des Reiteralm Gebirges: ein Beitrag zur Deckenfrage in den Berchtesgadener Alpen.- 107 S., Diss. LMU München, München

FISCHER, A. G. (1965): Eine Lateralverschiebung in den Salzburger Kalkalpen.- Verhandlungen der Geologischen Bundesanstalt, 1965, 20-33, Wien.

FORD, M., WILLIAMS, E. A., ARTONI, A., VERGES, J. & HARDY, S. (1997): Progressive evolution of a fault-related fold pair from growth strata geometries, Sant Llorens de Morunys, SE Pyrenees.- Journal of Structural Geology, 19, 413 - 441, Oxford.

FRANK, W. & SCHLAGER, W. (2006): Jurassic strike slip versus subduction in the Eastern Alps.- Int. Jour. Earth Sci., 95, 431-450, Stuttgart.

FROITZHEIM, N. & MANATSCHAL, G. (1996): Kinematics of Jurassic rifting, mantle exhumation, and passive-margin formation in the Austroalpine and Penninic nappes (eastern Switzerland).- Geological Society of America Bulletin, 108, 1120 - 1133, Boulder.

GARRISON, R. E. & FISCHER, A. G. (1969): Deep water limestones and radiolarites of the Alpine Jurassic.- In: FRIEDMANN, G. M. (Eds.), Depositional environments in carbonate rocks – a symposium, 20-56, Tulsa (SEPM Spec. Publ. 14).

GAWLICK, H.-J., AUBRECHT, R., SCHLAGINTWEIT, F., MISSONI, S. & PLASIENKA, D. (2015): Ophiolitic detritus in Kimmeridgian resedimented limestones and its provenance from an eroded obducted ophiolitic nappe stack south of the Northern Calcareous Alps (Austria).- Geologica Carpathica, 66, 473-487, Bratislava.

GAWLICK, H.-J., FRISCH, W., VECSEI, A., STEIGER, T. & BÖHM, F. (1999): The change from rifting to thrusting in the Northern Calcareous Alps as recorded in Jurassic sediments.- Geologische Rundschau, 87, 644 - 657, Stuttgart.

HAAS, J., KOVÁCS, S., KRYSTYN, L. & LEIN, R. (1995): Significance of Triassic facies zones in terrane reconstructions in the Alpine-North Pannonian domain.- Tectonophysics, 242, 19-40, Amsterdam.

HAHN, F. F. (1910): Die Geologie der Kammerkehr-Sonntagshorngruppe, I. Teil.- Jahrbuch der k. k. Geologischen Reichsanstalt, 60, 311-419, Wien.

HAHN, F. F. (1912): Versuch einer Gliederung der austroalpinen Masse westlich der österreichischen Traun.- Verhandlungen der Geologischen Reichsanstalt, 1912, 337-344, Wien.

HAHN, F. F. (1913a): Geologie des oberen Saalachgebietes zwischen Lofer und Diesbachtal.- Jahrbuch der k. k. Geologischen Reichsanstalt, 63, 1-76, Wien.

HAHN, F. F. (1913b): Grundzüge des Baues der nördlichen Kalkalpen zwischen Inn und Enns.- Mitteilungen der Österreichischen Geologischen Gesellschaft, 9, 374-500, Wien.

HANDY, M. R., M. SCHMID, S., BOUSQUET, R., KISSLING, E. & BERNOULLI, D. (2010): Reconciling plate-tectonic reconstructions of Alpine Tethys with the geological–geophysical record of spreading and subduction in the Alps.- Earth-Science Reviews, 102, 121-158, Amsterdam.

HORNSTEINER, G. (1991): Die jurassische Entwicklung auf der Waidringer Steinplatte unter besonderer Berücksichtigung der Scheiblberg Schichten an der Typlokalität.- unpublished Diploma thesis Univ. Innsbruck, 219 S., Innsbruck.

JACOBSHAGEN, V. & KOCH, K. E. (1959): Verkeilungen als Richtungsanzeiger an Überschiebungen.- Neues Jahrbuch für Geologie und Paläontologie, Monatshefte, 1959, 99-110, Stuttgart.

KRAINER, K., MOSTLER, H. & HADITSCH, J. G. (1994): Jurassische Beckenbildung in den Nördlichen Kalkalpen bei Lofer (Salzburg) unter besonderer Berücksichtigung der Manganerzgenese.- Abhandlungen der Geologischen Bundesanstalt, 50, 257 - 293, Wien.

LAVIER, L. L. & MANATSCHAL, G. (2006): A mechanism to thin the continental lithosphere at magma-poor margins.- Nature, 440, 324-328, London.

LEIN, R., SUZUKI, H. & GAWLIK, H.-J. (2009): Die Obersee-Brekzie bei Lunz (Niederösterreich): Revision der Stratigraphie und des Komponentenbestandes.- In: BRYDA, G. (Eds.), Arbeitstagung Blatt 101 Eisenerz: Leoben, 204-210, Wien (Geologische Bundesanstalt).

LINZER, H.-G., DECKER, K., PERESSON, H., DELL´MOUR, R. & FRISCH, W. (2002): Balancing lateral orogenic float of the Eastern Alps.- Tectonophysics, 354, 211-237, Amsterdam.

LUKESCH, M. E. (2003): Die Geologie des Nordwest-Randes der Berchtesgadener Masse bei Lofer (Nördliche Kalkalpen) - Genese oberjurassischer Brekzien und das Westende der Saalachtal Störung.- unpublished Diploma thesis Univ. Innsbruck, 127 S., Innsbruck.

MANDL, G. (2000): The Alpine sector of the Tethyan shelf - examples for Triassic to Jurassic sedimentation and deformation from the Northern Calcareous Alps.- Mitteilungen der Österreichischen Geologischen Gesellschaft, 92, 61-77, Wien.

MANDL, G. W. (2013): Zur Geologie des Raumes Hütteneckalm-Sandlingalm-Blaa-Alm (Salzkammergut, Österreich) mit kritischen Anmerkungen zur Sandlingalm-Formation.- Jahrbuch der Geologischen Bundesanstalt, 153, 33-74,

MISSONI, S. & GAWLICK, H.-J. (2010): Evidence for Jurassic subduction from the Northern Calcareous Alps (Berchtesgaden; Austroalpine, Germany).- International Journal of Earth Sciences, 100, 1605-1631, Stuttgart.

MOSNA, D. (2010): Die Lärchberg-Schichten im Gebiet des Gerhardsteins nahe Lofer - Dokumentation der Lärchberg-Schichten als Beitrag zur Interpretation der spätjurassischen Paläogeographie.- unpublished Diploma thesis Univ. Innsbruck, 120 S., Innsbruck.

MOSTLER, H. & KRAINER, K. (1993): Neue Ophiuren aus liassischen Slope-Sedimenten der Nördlichen Kalkalpen in der Umgebung von Lofer (Salzburg).- Geologisch-Paläontologische Mitteilungen Innsbruck, 19, 19-47, Innsbruck.

ORTNER, H. (2003): Cretaceous thrusting in the western part of the Northern Calcareous Alps (Austria) - evidences from synorogenic sedimentation and structural data.- Mitteilungen der Österreichischen Geologischen Gesellschaft, 94, 63-77, Wien.

ORTNER, H. (2017a): Geometry of growth strata in wrench-dominated transpression: 3D-model of the Upper Jurassic Trattberg rise, Northern Calcareous Alps, Austria.- Geophysical Research Abstracts, 19, EGU2017-9222,

ORTNER, H. (2017b): Tectonic maps in areas of deposition of exotic olistolithes – application to the Northern Calcareous Alps of Austria.- In: SARIC, K., PRELEVIC, D., SUDAR, M. & CVETKOVIC, V. (Eds.), 13th Workshop of Alpine Geological Studies, Zlatibor, Abstract volume, 79, Belgrade (Sapient Graphics).

ORTNER, H., AICHHOLZER, S., ZERLAUTH, M., PILSER, R. & FÜGENSCHUH, B. (2015): Geometry, amount and sequence of thrusting in the Subalpine Molasse of Western Austria and Southern Germany, European Alps.- Tectonics, 34, 1-30, Hoboken.

ORTNER, H., KOSITZ, A., WILLINGSHOFER, E. & SOKOUTIS, D. (2016): Geometry of growth strata in a transpressive fold belt in field and analogue model: Gosau Group at Muttekopf, Northern Calcareous Alps, Austria.- Basin Research, 28, 731–751, doi: 10.1111/bre.12129

ORTNER, H., USTASZEWSKI, M. & RITTNER, M. (2008): Late Jurassic tectonics and sedimentation: breccias in the Unken syncline, central Northern Calcareous Alps.- Swiss Journal of Geosciences, 101, Supplement 1, S55-S71, Basel.

PAVLIK, W. (2006): Provisorische Geologische Karte von Österreich, Blatt 92 - Lofer, GeoFAST 1:50.000.- Geologische Bundesanstalt, Wien.

PERESSON, H. & DECKER, K. (1997): The Tertiary dynamics of the northern Eastern Alps (Austria): changing palaeostresses in a collisional plate boundary.- Tectonophysics, 272, 125 - 157, Amsterdam.

PICOTTI, V. & COBIANCHI, M. (2017): Jurassic stratigraphy of the Belluno Basin and Friuli Platform: a perspective on far-field compression in the Adria passive margin.- Swiss Journal of Geosciences, 110, 833-850, Basel.

PILLER, W. E., EGGER, H., ERHART, C. W., GROSS, M., HARZHAUSER, M., HUBMANN, B., VAN HUSEN, D., KRENMAYR, H.-G., KRYSTYN, L., LEIN, R., LUKENEDER, A., MANDL, G. W., RÖGL, F., ROETZEL, G., RUPP, C., SCHNABEL, W., SCHÖNLAUB, H.-P. S., H., WAGREICH, M. & WESSELY, G. (2004): Die stratigraphische Tabelle von Österreich 2004 (sedimentäre Schichtfolgen).- (Kommission für die paläontologische und stratigraphische Erforschung Österreichs der Österreichische Akademie der Wissenschaften und Österreichische Stratigraphische Kommission).

PLÖCHINGER, B. (1953): Der Bau der südlichen Osterhorngruppe und die Thiton-Neokomtransgression.- Jahrbuch der Geologischen Bundesanstalt, 96, 257-273, Wien.

RASSER, M. W., VASICEK, Z., SKUPIEN, P., LOBITZER, H. & BOOROVA, D. (2003): Die Schrambach-Formation an ihrer Typuslokalität (Unter-Kreide, Nördliche Kalkalpen, Salzburg): Lithostratigraphische Formalisierung und "historische" Irrtümer.- In: PILLER, W. E. (Eds.), Stratigraphia Austriaca, Schriftenreihe der Erdwissenschaftlichen Kommission, 16, 193-216, Wien (Österreichische Akademie der Wissenschaften).

RATSCHBACHER, L., FRISCH, W., LINZER, G. & MERLE, O. (1991): Lateral extrusion in the Eastern Alps, Part 2: Structural analysis.- Tectonics, 10, 257 - 271, doi: 10.1029/90TC02623

RECHES, Z. & DIETERICH, J. H. (1983): Faulting of rocks in three-dimensional strain fields. I. Failure of rocks in polyaxial, servo-controlled experiments.- Tectonophysics, 95, 111-132, Amsterdam.

RITTNER, K. M. (2006): Geologie der östlichen Unkener Mulde am Kontakt zur Berchtesgadener Masse - Strukturgeologie und elektronische Verarbeitung geologischer Daten.- unpublished Diploma thesis Univ. Innsbruck, 104 S., Innsbruck.

ROSENBERG, C. L., BRUN, J.-P., CAGNARD, F. & GAPAIS, D. (2007): Oblique indentation in the Eastern Alps: Insights from laboratory experiments.- Tectonics, 26, TC2003, Washington, D.C.

SANDERS, D., LUKESCH, M., RASSER, M. & SKELTON, P. (2007): Shell beds of Diceratid rudists ahead of a low-energy gravelly beach (Thitonian, Northern Calcareous Alps, Austria): paleoecology and taphonomy.- Austrian Journal of Earth Sciences, 100, 186-199, Wien.

SCHEIDLEDER, A., BOROVICZENY, F., GRAF, W., HOFMANN, T., MANDL, G. W., SCHUBERT, G., STICHLER, W., TRIMBORN, P. & KRALIK, M. (2001): Pilotprojekt "Karstwasser Dachstein": Band 2: Karsthydrologie und Kontaminationsrisiko von Quellen.- Archiv für Lagerstättenforschung, 21, 1-155,

SCHLAGER, W. & SCHLAGER, M. (1973): Clastic sediments associated with radiolarites (Tauglbodenschichten, Upper Jurassic, Eastern Alps).- Sedimentology, 20, 65-89, Amsterdam.

SCHMID, S. M., BERNOULLI, D., FÜGENSCHUH, B., MATENCO, L., SCHEFER, S., SCHUSTER, R., TISCHLER, M. & USTASZEWSKI, K. (2008): The Alpine-Carpathian-Dinaride-orogenic system: correlation and evolution of tectonic units.- Swiss Journal of Geosciences, 101, 139-183, Basel.

SCHMID, S. M., FÜGENSCHUH, B., KISSLING, E. & SCHUSTER, R. (2004): Tectonic map and overall architecture of the Alpine orogen.- Eclogae Geologicae Helvetiae, 97, 93-117, Basel.

SCHWEIGL, J. & NEUBAUER, F. (1997): Structural evolution of the central Northern Calcareous Alps: Significance for the Jurassic to Tertiary geodynamics of the Alps.- Eclogae Geologicae Helvetiae, 90, 1 - 19, Basel.

SIEWERT, W. (1973): Zur Tektonik der nördlichen Ausläufer des Steinernen Meeres (Gebiet um den Hochkranz).- Verhandlungen der Geologischen Bundesanstalt, 1973, 255-265, Wien.

STAMPFLI, G. M. & BOREL, G. D. (2002): A plate tectonic model for the Paleozoic and Mesozoic constrained by dynamic plate boundaries and restored synthetic oceanic isochrons.- Earth and Planetary Science Letters, 196, 17-33, Amsterdam.

STEIGER, T. (1981): Kalkturbidite im Oberjura der Nördlichen Kalkalpen (Barmsteinkalke, Salzburg, Österreich).- Facies, 4, 215-348, Erlangen.

TOLLMANN, A. (1969): Tektonische Karte der Nördlichen Kalkalpen, 2. Teil: Der Mittelabschnitt.- Mitteilungen der Österreichischen Geologischen Gesellschaft, 61 (1968), 214-181, Wien.

TOLLMANN, A. (1976a): Analyse des klassischen nordalpinen Mesozoikums.- 580 S., Monographie der Nördlichen Kalkalpen, Teil II, Wien (Deuticke).

TOLLMANN, A. (1976b): Der Bau der Nördlichen Kalkalpen.- 449 S., Monographie der Nördlichen Kalkalpen, Teil III, Wien (Deuticke).

TOLLMANN, A. (1985): Geologie von Österreich, Band 2.- 710 S., Wien (Deuticke).

TRÜMPY, R. (1988): A possible Jurassic-Cretaceous transform system in the Alps and the Carpathians.- Geological Society of America Special Paper, 218, 93-109, Boulder.

VECSEI, A., FRISCH, W., PIRZER, M. & WETZEL, A. (1989): Origin and tectonic significance of radiolarian chert in the Austroalpine rifted continental margin.- In: HEIN, J. R. & OBRADOVIC, J. (Eds.), Siliceous Deposits of the Tethys and Pacific Regions, 65-80, New York (Springer).

VORTISCH, W. (1931): Tektonik und Breccienbildung in der Kammerkehr-Sonntagshorngruppe.- Jahrbuch der Geologischen Bundesanstalt, 80, 81-96, Wien.

WÄCHTER, J. (1987): Jurassische Massflow- und Internbrekzien und ihr sedimentär-tektonisches Umfeld im mittleren Abschnitt der nördlichen Kalkalpen.- Bochumer geol. und geotechn. Arbeiten, 27, 239 S., Bochum.

WEISSERT, H. J. & BERNOULLI, D. (1985): A transform margin in Mesozoic Tethys: evidence from the Swiss Alps.- Geologische Rundschau, 74, 665-679, Stuttgart.

WOLFGRUBER, S. (2010): Die Lärchberg-Schichten im Gebiet des Gerhardsteins nahe Lofer - Untersuchung der Schwermineralspektren der Loferer Schichten als Grundlage für einen möglichen Beitrag zur spätjurassischen Paläogeographie.- unpublished Diploma thesis Univ. Innsbruck, 107 S., Innsbruck.